Slow modal gating of single G protein-activated K^+ channels expressed in *Xenopus* oocytes

Daniel Yakubovich, Vassili Pastushenko*, Arkadi Bitler, Carmen W. Dessauer† and Nathan Dascal

*Department of Physiology and Pharmacology, Sackler School of Medicine, Tel Aviv University, Ramat Aviv 69978, Israel, *Institute of Biophysics, Johannes-Kepler University of Linz, A-4040 Linz, Austria and †Department of Integrative Biology, Pharmacology and Physiology, Medical School, University of Texas, Houston, TX 77030, USA*

(Received 30 November 1999; accepted 26 January 2000)

1. The slow kinetics of G protein-activated K^+ (GIRK) channels expressed in *Xenopus* oocytes were studied in single-channel, inside-out membrane patches. Channels formed by GIRK1 plus GIRK4 subunits, which are known to form the cardiac acetylcholine (ACh)-activated GIRK channel (K_{ACh}), were activated by a near-saturating dose of G protein $\beta\gamma$ subunits ($G_{\beta\gamma}$; 20 nM).

2. The kinetic parameters of the expressed GIRK1/4 channels were similar to those of cardiac K_{ACh}. GIRK1/4 channels differed significantly from channels formed by GIRK1 with the endogenous oocyte subunit GIRK5 (GIRK1/5) in some of their kinetic parameters and in a 3-fold lower open probability, P_o. The unexpectedly low P_o (0·025) of GIRK1/4 was due to the presence of closures of hundreds of milliseconds; the channel spent ~90 % of the time in the long closed states.

3. GIRK1/4 channels displayed a clear modal behaviour: on a time scale of tens of seconds, the $G_{\beta\gamma}$-activated channels cycled between a low-P_o mode (P_o of about 0·0034) and a bursting mode characterized by an ~30-fold higher P_o and a different set of kinetic constants (and, therefore, a different set of channel conformations). The available evidence indicates that the slow modal transitions are not driven by binding and unbinding of $G_{\beta\gamma}$.

4. The GTPγS-activated $G_{\alpha i1}$ subunit, previously shown to inhibit GIRK channels, substantially increased the time spent in closed states and apparently shifted the channel to a mode similar, but not identical, to the low-P_o mode.

5. This is the first demonstration of slow modal transitions in GIRK channels. The detailed description of the slow gating kinetics of GIRK1/4 may help in future analysis of mechanisms of GIRK gating.

The G protein-activated K^+ channels (GIRK, or Kir3, family) play important roles in the regulation of heartbeat and in inhibitory neurotransmission in the brain (for review, see Yamada *et al.* 1998). This is the only ion channel family whose members are known to be activated by G protein $\beta\gamma$ subunits ($G_{\beta\gamma}$) by a direct protein–protein interaction (reviewed by Kurachi, 1995; Wickman & Clapham, 1995; Dascal, 1997; Jan & Jan, 1997). Theoretically, this provides a unique opportunity to study the molecular details of the interaction of $G_{\beta\gamma}$ with its effector with millisecond resolution and, from there, to understand better the mechanisms of G protein–effector interactions in general. However, the high density of channels in cardiac and neuronal cells, in which GIRK channels are endogenously expressed, makes it difficult to obtain patches with one channel. This precluded a comprehensive description of the closed states and hampered the study of the slow kinetic properties of GIRK gating. In this study, we utilized the potential of a heterologous expression system, the *Xenopus* oocyte, in which the channel density in the membrane can be controlled by regulating the level of expression, to overcome this problem.

The GIRK family includes GIRK1, which was initially cloned from atrium (Dascal *et al.* 1993; Kubo *et al.* 1993), and additional subunits (GIRK2 to GIRK5). In most cases, functional GIRK channels are heterotetramers formed by GIRK1 with the other subunits: GIRK2, GIRK3 and GIRK4 in the brain (Lesage *et al.* 1994, 1995; Duprat *et al.*

1995; Kofuji *et al.* 1995; Spauschus *et al.* 1996), and GIRK4 in the atrium (Krapivinsky *et al.* 1995; Lesage *et al.* 1995; Chan *et al.* 1996*a*). Each GIRK1 plus GIRK2 or GIRK4 heterotetramer contains two GIRK1 and two GIRK2 or GIRK4 subunits (Inanobe *et al.* 1995; Silverman *et al.* 1996; Corey *et al.* 1998). GIRK2 and GIRK4 also appear to form functional homotetrameric channels in brain and heart, respectively (Liao *et al.* 1996; Corey *et al.* 1998). GIRK1 alone is unable to form functional channels but, in *Xenopus* oocytes, it assembles with an endogenous subunit, GIRK5, forming functional GIRK1/5 channels (Hedin *et al.* 1996).

So far there are several reports on the single-channel kinetics of GIRK (also called K_{ACh}) channels in atrial and sinoatrial node cells (Sakmann *et al.* 1983; Kim, 1991; Ivanova-Nikolova & Breitwieser, 1997; Ivanova-Nikolova *et al.* 1998; Nemec *et al.* 1999), in neurons (Grigg *et al.* 1996), and in *Xenopus* oocytes expressing GIRK1/4 channels (composed of GIRK1 plus GIRK4 subunits) (Chan *et al.* 1996*a*; Kim *et al.* 1997). Limited analyses of the single-channel parameters of GIRK1/2 (Kofuji *et al.* 1995) and GIRK1/5 (Slesinger *et al.* 1995; Luchian *et al.* 1997) channels in *Xenopus* oocytes are also available. In all cases, in the presence of ATP, GIRK shows at least two open states with time constants of 1–1·4 and 3–6 ms. There is no consensus about the number and properties of closed states since, as mentioned above, they could not be reliably estimated from the multichannel patches. Despite this, there is a general agreement that openings of agonist-, GTPγS- or $G_{\beta\gamma}$-activated channels are clustered in bursts (Sakmann *et al.* 1983; Kirsch & Brown, 1989; Slesinger *et al.* 1995; Ivanova-Nikolova & Breitwieser, 1997; Luchian *et al.* 1997; Ivanova-Nikolova *et al.* 1998; Nemec *et al.* 1999). At present, no consensus definition of a burst is available due to the problem of estimation of inter-burst closed times (Colquhoun & Hawkes, 1995) and the possibility that bursts of GIRK openings may be organized in clusters (see Dascal, 1997).

Recently, Ivanova-Nikolova and colleagues (Ivanova-Nikolova & Breitwieser, 1997; Ivanova-Nikolova *et al.* 1998) presented evidence for modal gating of cardiac GIRK channels (K_{ACh}, presumably GIRK1/4). A mode is assumed to correspond to a specific set of conformations of the channel molecule characterized by a defined number of open and closed states and, correspondingly, a characteristic set of kinetic parameters (Hess *et al.* 1984; Delcour *et al.* 1993; Delcour & Tsien, 1993; Keynes, 1994). A shift from one mode to another (i.e. from one set of conformations to another) may be promoted by a modulatory molecule, changes in voltage, phosphorylation, etc. (Hess *et al.* 1984; Imredy & Yue, 1994; Smith & Ashford, 1998). Slow 'cycling' of the channels between the different modes on a scale of many seconds is an important characteristic of modal gating (Zhou *et al.* 1991; Delcour & Tsien, 1993; Keynes, 1994). Ivanova-Nikolova and colleagues proposed the existence of three modes (frog atrium; Ivanova-Nikolova & Breitwieser, 1997) or five modes (rat atrium; Ivanova-Nikolova *et al.* 1998); high concentrations of agonist (ACh) or $G_{\beta\gamma}$ promote the shift to modes with high open probability, P_o, characterized by both a higher frequency of openings and a longer open time. A model has been proposed in which the transitions between the modes are driven by the number of $G_{\beta\gamma}$ molecules bound to each channel molecule. At present, this model remains incomplete, because kinetic parameters of the channel states within the modes have not been characterized, channel behaviour over a long time scale has not been analysed, and discrepancies between ACh- and $G_{\beta\gamma}$-induced modes were detected (Ivanova-Nikolova *et al.* 1998). Therefore, modal gating of GIRK channels is in need of better characterization.

While studying single GIRK channels expressed in *Xenopus* oocytes, after activation by near-saturating concentrations of purified $G_{\beta\gamma}$, we observed transitions from a bursting behaviour (which lasted for many seconds) to a pattern with low probability of opening characterized by single openings or short bursts. From a large number of records of GIRK1/5 and GIRK1/4 channels activated by $G_{\beta\gamma}$, we selected those which undoubtedly were from only a single channel, and analysed their kinetics. With both subunit compositions, the GIRK channels showed a rich abundance of closed states. Very long closures of hundreds of milliseconds, previously never described, accounted for up to 90% of the total time of channel activity and this was the reason for the low P_o. On a time scale of tens of seconds, the $G_{\beta\gamma}$-activated GIRK1/4 channels cycled between a low-P_o mode (P_o of about 0·0034) and a bursting mode characterized by an ~30-fold higher P_o and a different set of kinetic constants. This is the first demonstration of slow modal transitions in GIRK channels. The relationship between these kinetic modes and the ones described by Ivanova-Nikolova and collaborators (Ivanova-Nikolova *et al.* 1998) is unclear at present.

METHODS

Preparation of oocytes and RNA

The oocytes were prepared as previously described (Dascal & Lotan, 1992). Briefly, female *Xenopus laevis* frogs, maintained at 20 ± 2 °C on an 11 h light–13 h dark cycle, were anaesthetized in a 0·15% solution of procaine methanesulfonate (MS222), and portions of ovary were removed through a small incision on the abdomen. The incision was sutured, and the animal was returned to a separate tank until it had fully recovered from the anaesthesia, and afterwards was returned to a large tank where, together with the other postoperational animals, it was allowed to recover for at least 4 weeks until the next surgery. The animals did not show any signs of postoperational distress. All the experiments were carried out in accordance with the Tel Aviv University Institutional Animal Care and Use Committee (permit nos 4-96-50 and 11-99-47). The oocytes were defolliculated by collagenase treatment and injected with 50 nl of RNA solution each (see below). After RNA injection, oocytes were incubated for 2–5 days at 20–22 °C in NDE-96 solution (96 mM NaCl, 2 mM KCl, 1 mM $MgCl_2$, 1 mM $CaCl_2$, 2·5 mM sodium pyruvate, 50 μg ml^{-1} gentamicine, 5 mM Hepes, pH 7·5).

cDNA plasmid clones were linearized with the appropriate restriction enzymes, as previously described: GIRK1 (Dascal *et al.* 1993),

muscarinic m2 receptor (m_2R; Dascal *et al.* 1993), GIRK4 (rcKATP; Ashford *et al.* 1994). RNA was transcribed *in vitro* from the linearized plasmid templates, using a standard procedure (Dascal & Lotan, 1992). When both GIRK1 and GIRK4 were expressed, oocytes were injected with equal amounts (by weight) of the mRNAs of the two subunits. m_2R RNA (100–200 pg oocyte^{-1}) was not always present; the activation of the channel by $G_{\beta\gamma}$ did not depend on the expression of the receptor.

Reagents and solutions

Pipette solution contained (mM): 144 KCl, 2 NaCl, 1 $MgCl_2$, 1 $CaCl_2$, 0·1–1 $GdCl_3$ and 10 Hepes-KOH, pH 7·5. Bath solution contained (mM): 140 KCl, 6 NaCl, 4 $MgCl_2$, 1 EGTA, 0·1 GDPβS, 2 Na-ATP and 10 Hepes-KOH, pH 7·5.

Prenylated $G_{\beta1\gamma2}$ was prepared as described by Iniguez-Lluhi *et al.* (1992) and Kozasa & Gilman (1995) and stored in 3–5 μl aliquots at a concentration of 20–100 μM at −80 °C for up to 3 years without appreciable loss of activity. During the experiments, an aliquot of $G_{\beta\gamma}$ was thawed at 30 °C and stored on ice for up to 6 h. Two to eight minutes after patch excision, 0·5–2 μl of the $G_{\beta1\gamma2}$ stock solution was diluted into 50 μl of the bath solution, then added to the bath and mixed. Recombinant myristoylated $G_{\alpha i1}$ protein was prepared as described by Linder *et al.* (1991) and activated by incubation with 50 mM Na-Hepes (pH 8·0), 10 mM $MgSO_4$, 1 mM EGTA, 2 mM DTT and 400 μM GTPγS for 30 min. Free GTPγS was removed by gel filtration in G_α buffer (20 mM Na-Hepes (pH 8·0), 2 mM $MgSO_4$, 1 mM EDTA, 2 mM DTT) and the protein was dissolved in the G_α buffer at a concentration of 20 or 40 μM. Frozen $G_{\alpha i1}$ was shipped in dry ice in 20–100 μl aliquots from Texas to Tel Aviv, where it was thawed at 30 °C, further diluted to a final concentration of 2·5 μM in the G_α buffer, divided into 2–10 μl aliquots in siliconized Eppendorf tubes, refrozen in liquid N_2, and stored at −80 °C. In the course of an electrophysiological experiment, an aliquot was thawed at 30 °C, placed on ice, diluted in G_α buffer if necessary, then applied to the bath no longer than 5 min after thawing together with $G_{\beta1\gamma2}$ (Schreibmayer *et al.* 1996). We noticed that the efficiency of $G_{\alpha i1}$ in blocking the GIRK channels decreased within several months of storage. Therefore, $G_{\alpha i1}$ protein was used within 2–4 months of activation with GTPγS.

Organic materials were from Sigma, unless indicated otherwise. All inorganic substances were of analytical or molecular biology grade.

Single-channel measurements

Pipettes were made from borosilicate glass (usually LE-16, Dagan Corp., Minneapolis, MN, USA) and had resistances of 0·8–2·5 MΩ. The oocyte vitelline membrane was removed in the bath solution, and the oocytes were immediately transferred to the experimental bath filled with 500 μl of bath solution. After seal formation, the patches were excised and exposed to air to prevent the formation of closed membrane vesicles at the tip. The basal activity of the channel was recorded for at least 1 min after air exposure, and then $G_{\beta\gamma}$ or $G_{\beta\gamma}$ together with $G_{\alpha i1}$ were added. Currents were recorded with an Axopatch 200A amplifier (Axon Instruments Inc.) at −80 mV, filtered at 2 kHz with the internal 4-pole Bessel filter of the Axopatch 200A, sampled at 2·5 or 4 kHz and stored on the hard disk of an IBM-compatible personal computer using Axotape software (Axon Instruments). The inward rectification (a hallmark of GIRK, as opposed to the endogenous stretch-activated channels which do not show inward rectification) was verified by comparing records at −80 and +80 mV. The concentrations of $GdCl_3$ used (0·1 mM or, more often, 1 mM) completely inhibited the stretch-activated channels. The recordings were made at 20–22 °C.

Data analysis

The number of channels in patch was estimated from the number of overlaps observed during recording in the presence of 20 mM $G_{\beta\gamma}$. For single-channel analyses, only patches with no overlapping openings during the whole period of recording (6–11 min) were included in the analysis. In some GIRK1/5 channel records, a subconductance state of about 60% of the main conductance was observed; it appeared only between the bursts of the main conductance state and never accounted for more than 2·5% of the total open time (D. Yakubovich, V. Pastushenko & N. Dascal, unpublished observations). Only records in which these subconductance openings contributed to less than 1·7% of the total measured open time have been selected for analysis here (9 out of 13 single-channel records).

For closed and open time analysis, event lists were generated using Fetchan 6 software (Axon Instruments) based on a 50% criterion. In different experiments, the total number of events varied between 5000 and 40 000. The event lists were imported into Matlab for Windows (version 4.2c.1, Matworks Inc.) and further analysed using software written for this purpose, as explained below. Closed and open time distributions were generated from the event lists in the all-points histogram form, with a basic bin width equal to the sampling interval (0·25 or 0·4 ms). To avoid empty bins linear bins of variable length were introduced:

$$t_i = t_{i,\mathrm{mid}} - t_{i-1,\mathrm{mid}}, \tag{1}$$

where t_i is the width, in milliseconds, of the ith non-empty bin, $t_{i,\mathrm{mid}}$ is the midpoint of this bin, and $t_{i-1,\mathrm{mid}}$ is the midpoint of the preceding non-empty bin. For relatively short openings and closures, all 'basic' bins were populated and the basic bin width was preserved, but for very long openings and closures (which were relatively rare), the bin width was significantly longer. The histogram was then transformed into a probability density form using eqn (2):

$$\mathrm{p.d.}_i = n_i / t_i \Sigma n_i, \tag{2}$$

where $\mathrm{p.d.}_i$ is the probability density of the ith bin, t_i is the bin width in milliseconds and n_i is the number of events in the bin. Probability density distributions were fitted to the standard form of the probability density function with N exponents:

$$\mathrm{p.d.f.} = \sum_{k=1}^{N} a_k \tau_k^{-1} \exp(-t/\tau_k), \tag{3}$$

where a_k, or 'weighting factor', is the contribution of a kth exponential component to the total area below the fitted curve (and thus $\Sigma a_k = 1$), t is time, and τ_k is the characteristic time constant of the kth component (Colquhoun & Hawkes, 1995). Correction for missing (short) events was made assuming that events shorter than half the sampling interval are unobservable (see Colquhoun & Sigworth, 1995). No interpolation of dwell times between bins was used in the fitting procedures. The fits were made utilizing the maximum likelihood method. Note that, for clarity of presentation, in the figures the probability density distributions and the results of the fitting procedures are presented on a log–log scale or with logarithmic time bins (e.g. Fig. 1), although the data were always fitted using linear bins, as explained above.

Mean open or closed time ($t_{o,k}$ or $t_{c,k}$, respectively) of the kth exponential component was calculated as described by Colquhoun & Sigworth (1995):

$$t_{o,k} = a_{o,k} \tau_{o,k}, \tag{4a}$$

$$t_{c,k} = a_{c,k} \tau_{c,k}. \tag{4b}$$

The mean open and closed times of the whole distribution, t_o and t_c, are the sums of open and closed times of all N components (Colquhoun & Sigworth, 1995):

$$t_o = \sum_{k=1}^{N} t_{o,k}, \quad (5a)$$

$$t_c = \sum_{k=1}^{N} t_{c,k}. \quad (5b)$$

The single-channel open probability, P_o, observed in the experiment was obtained using the straightforward definition:

$$P_o = T_o/(T_o + T_c), \quad (6)$$

where T_o is the total time the channel was open during the whole period of the experiment, and T_c is the total time the channel was closed. The total recording time is $T_o + T_c$.

P_o can also be calculated when one knows the mean open and closed times (t_o and t_c, respectively). By definition, $t_o = T_o/N_o$, where N_o is the total number of open events. Similarly, $t_c = T_c/N_c$. Since N_o and N_c differ at most by 1, for all practical reasons in an experiment with hundreds of recorded events $N_o = N_c$, and thus t_o and t_c are proportional to the total time the channel is open or closed, respectively. Hence:

$$P_o = t_o/(t_o + t_c). \quad (7)$$

Accordingly, the contribution of a population of openings to the total mean open time, $C_{o,k}$, is given by:

$$C_{o,k} = t_{o,k}/t_o; \quad (8a)$$

the same applies to closed times:

$$C_{c,k} = t_{c,k}/t_c. \quad (8b)$$

Analysis of frequencies of openings ('frequency analysis') was performed as described by Ivanova-Nikolova *et al.* (1998). The record was divided into 0·4 s segments, and the frequency of opening, $f_{o,s}$ (n_s (0·4 s)$^{-1}$, in Hz, where n_s is the number of openings in the segment), and the open probability, $P_{o,s}$ ($T_{o,s}$ (0·4 s)$^{-1}$, where $T_{o,s}$ is the total open time within the segment), within each segment were calculated using pSTAT 6 software (Axon Instruments). The results were exported as ASCII files, combined from several cells and/or parts of records as explained in the text, and, if desired, presented in the form of histograms. The resulting frequency distributions (e.g. Figs 3*D* and 5*C* and *D*) were fitted as described by Colquhoun & Hawkes (1981) using a non-linear least squares algorithm (Sigmaplot, Jandel Corp.).

Data presentation and statistical analysis

Whenever average values were calculated, they are presented as means ± S.E.M. For comparison of two groups, a normality test was performed and, in accordance, Mann-Whitney rank sum test or Student's unpaired t test were utilized. Comparison of several groups with one control group (Fig. 7) was done by one-way ANOVA followed by Dunnet's test.

RESULTS

Single-channel kinetics of GIRK1/5 and GIRK1/4 channels

Injection of GIRK1 RNA causes the appearance of functional GIRK channels in *Xenopus* oocytes (Dascal *et al.* 1993; Kubo *et al.* 1993), due to the presence of endogenous GIRK5 protein which forms heteromers with GIRK1 (Hedin *et al.* 1996). The GIRK1/5 channels are a convenient model for investigation because their low density in oocyte membrane, most probably the result of a limited availability of GIRK5, allows the selection of records with a single channel. Therefore, we started this study with a kinetic analysis of GIRK1/5. Oocytes were injected with 500–1000 pg GIRK1 RNA, which always gave a maximal attainable expression of GIRK1/5 current in whole-cell recordings (Vorobiov *et al.* 1998; data not shown). GIRK activity was measured in inside-out patches with ~150 mM KCl on both sides of the membrane, and with 6 mM NaCl, 4 mM $MgCl_2$ and 2 mM ATP in the bath. These conditions ensure that there will be no 'rundown' of the membrane phosphatidylinositol bisphosphate (PIP_2), which is necessary for channel activity (Sui *et al.* 1998; Huang *et al.* 1998). It should be noted that recordings in cell-attached patches with ACh in the pipette (data not shown) revealed two features that undermined a meaningful single-channel analysis. First, even when the patch appeared to be a single-channel one, further excision into bath solution containing GTPγS or $G_{\beta\gamma}$ increased the channel open probability (P_o) and usually revealed the presence of more than one channel. Second, at high concentrations of ACh (10 μM) the P_o was often lower, and the mean closed time longer, than with low concentrations of ACh (10–100 nM), suggesting the involvement of an agonist-evoked desensitization process, which has been well described both in atrial cells and in oocytes (Bunemann *et al.* 1996; Vorobiov *et al.* 1998). Therefore, we chose to analyse channel gating in excised patches using purified $G_{\beta\gamma}$, which did not cause time-dependent desensitization (see below, Figs 1 and 2) and gave a higher P_o, ensuring real single-channel recordings (see Discussion).

Both in the cell-attached configuration and after patch excision, without any agonist in the pipette, very low levels of basal activity were observed. In patches later verified as containing a single channel, as few as one to four openings per minute were often observed. Addition of 20 nM purified recombinant $G_{\beta1\gamma2}$ was followed, after 0·2–2 min, by a robust activation of the channel (Fig. 1*A*; cf. Schreibmayer *et al.* 1996) characterized by bursts of openings separated by periods of variable duration during which no openings were detected (Fig. 1*Ab* and *Ac*). After full activation by $G_{\beta\gamma}$ (as judged by eye), the recording was continued without interruption at −80 mV for 6–11 min. Zero to four channels were usually present per patch, with electrodes of 1–1·8 MΩ resistance (inner diameter, 3·5–2·5 μm). Thirteen out of fifty patches that showed activation by $G_{\beta\gamma}$ contained a single channel.

For kinetic analysis, we selected nine recordings in which there was no overlap of openings during the whole time of the record. Selection by this criterion ensures, with a high level of confidence, the presence of a single channel in the patch (see Discussion). Each of the recordings was subjected to a kinetic analysis in the Matlab environment using the procedure described in the Methods. An example of such analysis is shown in Fig. 1. Open time distribution, presented

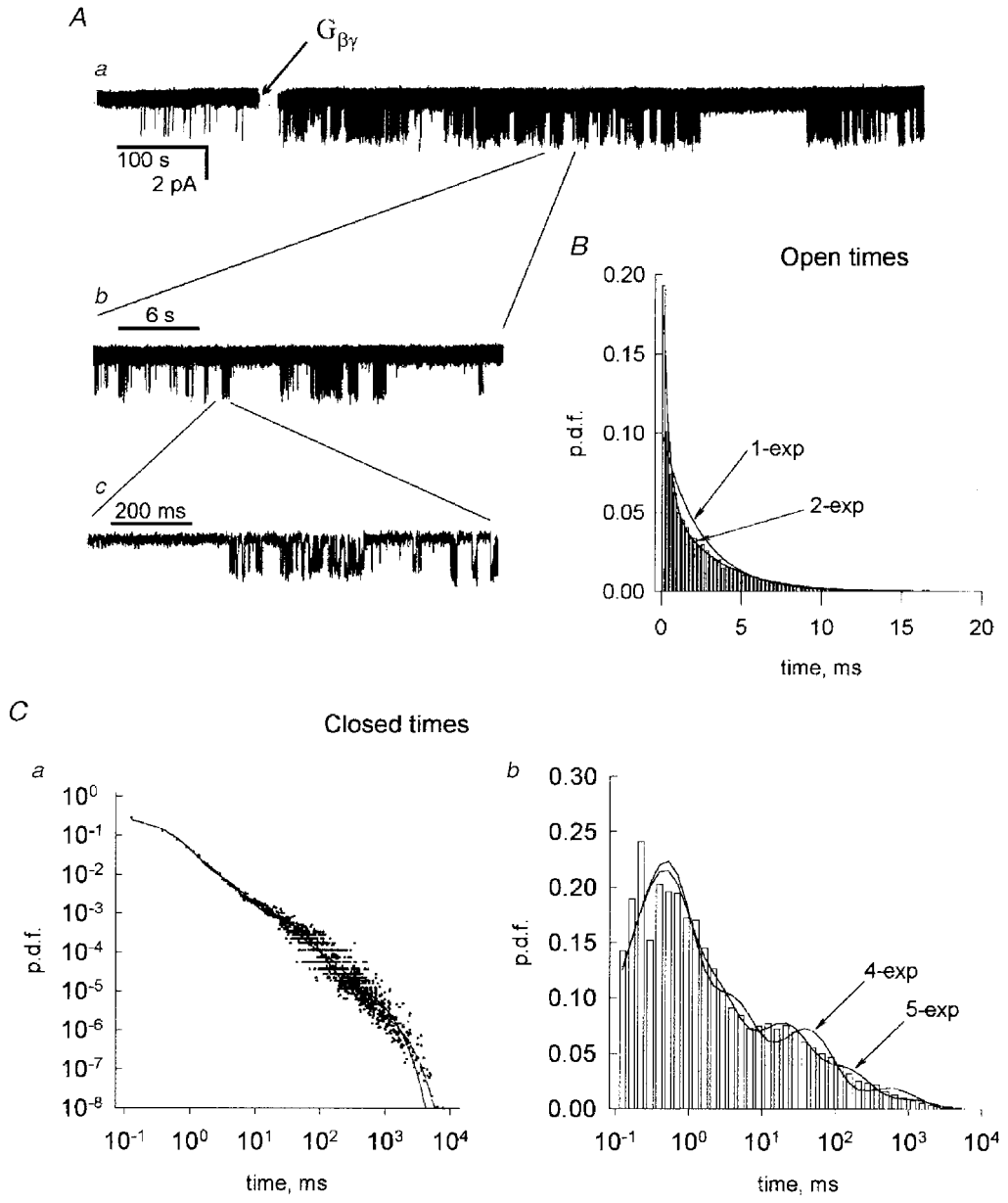

Figure 1. Analysis of the kinetics of a GIRK1/5 channel activated by 20 nM $G_{\beta\gamma}$ in a representative patch

A, record of GIRK1/5 activity. Trace *a* shows the full time course of the experiment, starting after excision of the patch. The arrow indicates addition of 20 nM $G_{\beta\gamma}$ ~2·5 min after excision (the record during the time of addition of $G_{\beta\gamma}$ has been blanked out). Traces *b* and *c* show details of channel activity on expanded time scales. Inward K^+ currents are shown as downward deflections in this and the following figures. *B*, open time distribution: linear histogram in the p.d.f. form and one- and two-exponential fits. A total of > 18 000 events were analysed. The continuous lines were drawn using the following parameters: for one-exponential fit, $\tau = 2{\cdot}44$ ms; for two-exponential fit, $\tau_{o1} = 0{\cdot}37$ ms, $a_{o1} = 0{\cdot}24$; $\tau_{o2} = 3{\cdot}09$ ms, $a_{o2} = 0{\cdot}76$. *Ca*, closed time distribution in the p.d.f. form with linear bins, and four- and five-exponential fits (continuous and dashed lines, respectively). A total of >18 000 events were analysed. Note that the logarithmic time scale is used here only for clarity of presentation (see Methods). For four-exponential fit, $\tau_{c1} = 0{\cdot}42$ ms, $a_{c1} = 0{\cdot}518$; $\tau_{c2} = 2{\cdot}91$ ms, $a_{c2} = 0{\cdot}24$; $\tau_{c3} = 37{\cdot}24$ ms, $a_{c3} = 0{\cdot}19$; $\tau_{c4} = 538{\cdot}59$ ms, $a_{c4} = 0{\cdot}0517$; for five-exponential fit, $\tau_{c1} = 0{\cdot}36$ ms, $a_{c1} = 0{\cdot}44$; $\tau_{c2} = 1{\cdot}62$ ms, $a_{c2} = 0{\cdot}27$; $\tau_{c3} = 16{\cdot}1$ ms, $a_{c3} = 0{\cdot}18$; $\tau_{c4} = 110{\cdot}6$ ms, $a_{c4} = 0{\cdot}09$; $\tau_{c5} = 874$ ms, $a_{c5} = 0{\cdot}02$. *Cb*, closed time histogram with logarithmic bins; the curves were drawn using the results of the fitting procedure shown in *a*. For presentation purposes, the first two bins were subdivided into smaller ones, and the numbers of events in each bin were interpolated.

Table 1. Kinetic parameters obtained from single-channel analyses of GIRK1/5 and GIRK1/4 channels

	GIRK1/5 (9 cells)	GIRK1/4 (4 cells)	GIRK1/4		GIRK1/4 + $G_{\alpha i1}$ (4 cells)
			Burst mode	Low-P_o mode	
Open times					
τ_{o1} (ms)	0·81 ± 0·11	0·71 ± 0·01	1·24	0·50	0·57
t_{o1} (ms)	0·23 ± 0·04	0·38 ± 0·05	0·86	0·41	0·35
a_{o1}	0·30 ± 0·04	0·52 ± 0·06	0·698	0·81	0·605
τ_{o2} (ms)	5·00 ± 0·80	2·86 ± 0·52	4·07	2·63	3·59
t_{o2} (ms)	3·43 ± 0·52	1·40 ± 0·36 *	1·23	0·50	1·42
a_{o2}	0·70 ± 0·04	0·47 ± 0·06	0·302	0·19	0·395
Total t_o (ms)	3·85 ± 0·55	1·98 ± 0·32	2·09	0·91	1·77
Closed times					
τ_{c1} (ms)	0·54 ± 0·04	0·62 ± 0·02	0·67	0·93	0·78
t_{c1} (ms)	0·27 ± 0·03	0·22 ± 0·02	0·30	0·22	0·34
a_{c1}	0·503 ± 0·046	0·355 ± 0·029	0·444	0·239	0·438
τ_{c2} (ms)	3·97 ± 0·55	4·9 ± 0·95	5·67	—	—
t_{c2} (ms)	0·64 ± 0·08	1·41 ± 0·38	2·36	—	—
a_{c2}	0·171 ± 0·018	0·279 ± 0·051 *	0·415	—	—
τ_{c3} (ms)	35·7 ± 5·05	31·4 ± 3·7	46·6	23·3	14·4
t_{c3} (ms)	8·33 ± 2·04	6·73 ± 1·42	5·83	8·29	4·66
a_{c3}	0·208 ± 0·030	0·209 ± 0·019	0·125	0·356	0·324
τ_{c4} (ms)	236 ± 61·4	240·4 ± 31	—	238·5	314·1
t_{c4} (ms)	18·6 ± 2·5	31·3 ± 7·2	—	84·1	48·5
a_{c4}	0·104 ± 0·014	0·128 ± 0·026	—	0·352	0·154
τ_{c5} (ms)	1432 ± 215	2200 ± 403	760	2637	6703
t_{c5} (ms)	15·2 ± 2·2	54·6 ± 19·4 *	11·87	138·7	561·3
a_{c5}	0·013 ± 0·002	0·029 ± 0·012	0·016	0·053	0·084
Total t_c (ms)	43·4 ± 5·6	94·3 ± 25·2 *	20·3	231·3	614·8

Data in the burst and low-P_o modes were pooled from all cells ($n = 4$) before the analysis. * Statistically significant difference from GIRK1/5 ($P < 0·05$).

as a probability density function (p.d.f.) histogram in Fig. 1*B*, could be well fitted to a biexponential function, with time constants (τ_{o1} and τ_{o2}) of ~0·8 and 5 ms (see Table 1 for details). Fitting with a single exponential did not satisfactorily describe the data.

The closed time distribution was significantly more complex. This distribution is presented in Fig. 1*Ca* in the form in which the actual fitting procedure was performed (with linear time bins of variable length; see Methods) and in the more conventional form of a histogram with logarithmic time bins in Fig. 1*Cb*. Exponential fits of the data to a probability density function were done using a maximal likelihood algorithm with two, three, four or five exponents. At least four exponential components were required to describe this distribution, but the five-exponential fit was visibly better in most cells (Fig. 1*Cb*). The characteristic time constants τ_{c1} to τ_{c5} were, on average, approximately 0·5, 4, 36, 236 and 1432 ms (Table 1). (A few very long closures of > 10 s, such as the one in Fig. 1*Aa*, were excluded from the fit in a few cells. They might represent an additional population of closures, but were too infrequent for a reliable fit.)

GIRK1/4 channels were studied in oocytes injected with much smaller, equal amounts of GIRK1 and GIRK4 RNA (25–100 pg oocyte^{-1}). It is important to emphasize that, when GIRK1 RNA was injected alone at these concentrations, the whole-cell currents were very small (Vorobiov *et al.* 1998), and we were usually unable to detect any GIRK channel activity with patch electrodes of 1–1·8 MΩ resistance. In contrast, when GIRK4 was coexpressed, even these small amounts of RNA gave rise to whole-cell currents of several microamps (not shown). Several channels were usually activated by 20 nM $G_{\beta\gamma}$ in small patches (pipettes of 1·5–2·5 MΩ resistance, 2·7–1·5 μm inner diameter), and single-channel records were obtained in only four out of > 70 patches. Each of the four single-channel records was analysed separately.

The general pattern of GIRK1/4 activity was similar to that of GIRK1/5 (Fig. 2*A*). Open time distribution could be satisfactorily fitted by a biexponential function with time constants of 0·7 and 2·9 ms (Fig. 2*B* and Table 1). Like GIRK1/5, at least four exponents were necessary to describe the closed time distribution, but the fit was

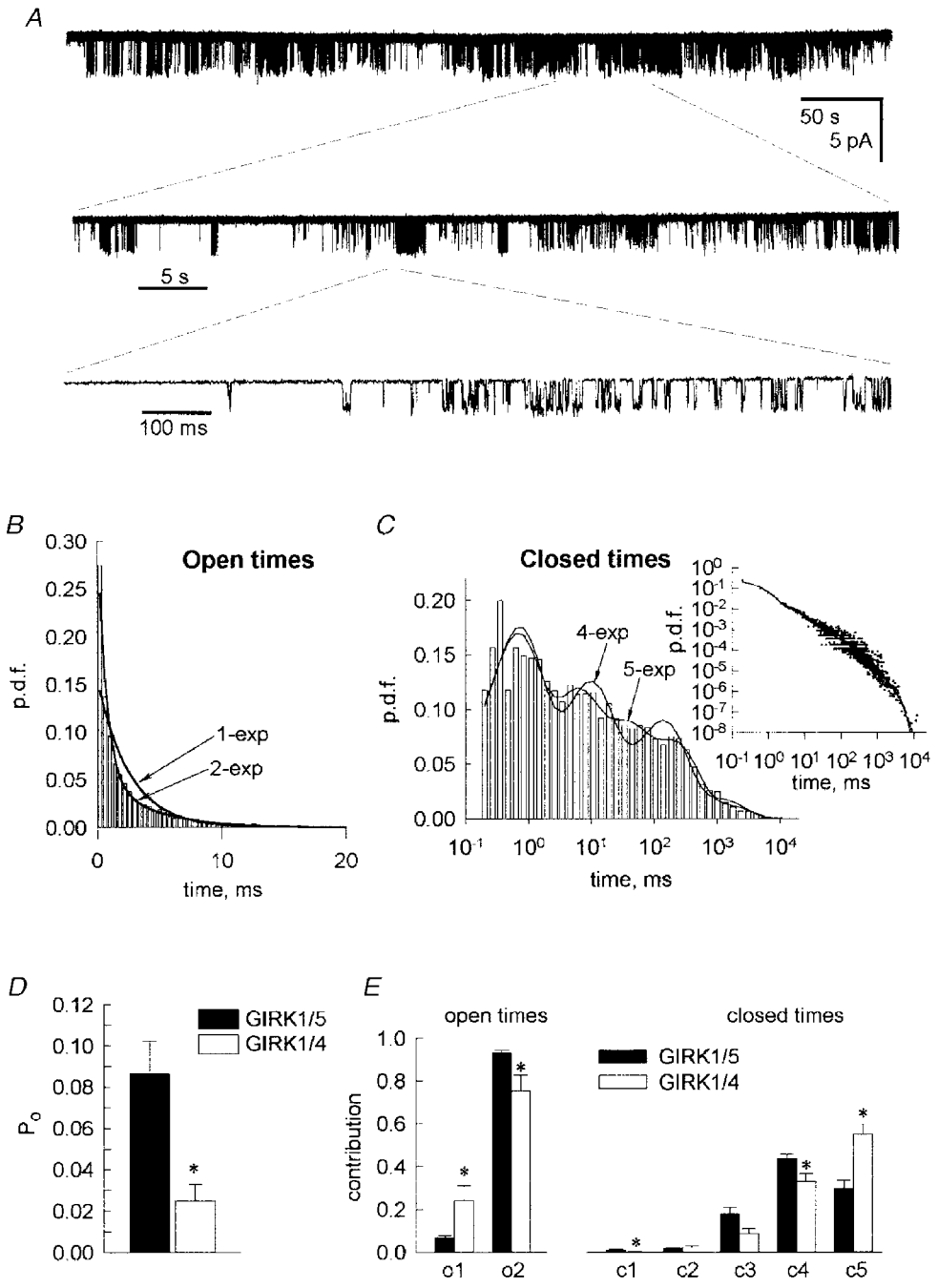

Figure 2. Analysis of the kinetics of a GIRK1/4 channel activated by 20 nM $G_{\beta\gamma}$ in a representative patch

A, record of channel activity after activation by 20 nM $G_{\beta\gamma}$. $G_{\beta\gamma}$ was applied about 1 min before the beginning of the upper trace. The end of the upper trace corresponds to the time when the experiment was terminated. The middle and lower traces show segments of the record on an expanded time scale. *B*, open time distribution in the p.d.f. form. A total of > 5500 events were analysed. For one-exponential fit, $\tau = 2{\cdot}58$ ms; for two-exponential fit, $\tau_{o1} = 0{\cdot}69$ ms, $a_{o1} = 0{\cdot}451$; $\tau_{o2} = 4{\cdot}14$ ms, $a_{o2} = 0{\cdot}548$. *C*, closed time distribution. Total of > 5500 events were analysed. The closed time histogram with logarithmic time bins was drawn using the parameters of the p.d.f. fit (see inset), as explained in Fig. 1*C*. The inset shows a probability density plot and four- and five-exponential fits in the p.d.f. form. For four-exponential fit, $\tau_{c1} = 0{\cdot}63$ ms, $a_{c1} = 0{\cdot}417$; $\tau_{c2} = 8{\cdot}56$ ms, $a_{c2} = 0{\cdot}302$; $\tau_{c3} = 129{\cdot}5$ ms, $a_{c3} = 0{\cdot}231$; $\tau_{c4} = 1085$ ms, $a_{c4} = 0{\cdot}049$; for five-exponential fit, $\tau_{c1} = 0{\cdot}564$ ms, $a_{c1} = 0{\cdot}377$; $\tau_{c2} = 4{\cdot}58$ ms, $a_{c2} = 0{\cdot}235$; $\tau_{c3} = 26{\cdot}32$ ms, $a_{c3} = 0{\cdot}172$; $\tau_{c4} = 190$ ms, $a_{c4} = 0{\cdot}183$; $\tau_{c5} = 1352$ ms, $a_{c5} = 0{\cdot}033$. *D*, open probabilities of GIRK1/5 and GIRK1/4 channels activated by 20 nM $G_{\beta\gamma}$. *E*, contribution of components of distributions of open and closed times to total open and closed times. In *D* and *E*, the asterisks indicate statistically significant differences ($P < 0{\cdot}05$).

substantially improved by using a five-exponential function (Fig. 2*C*). The values of the closed time constants τ_{c1} to τ_{c5} were similar to those of GIRK1/5. The fraction of the total area under the fitted curve (a_k) of the second component was significantly different (Table 1).

The most striking difference between GIRK1/4 and GIRK1/5 was an ~3-fold lower P_o of GIRK1/4 (Fig. 2*D*). To understand the factors determining the low P_o of GIRK1/4, the results were further processed as explained in the Methods (eqns (4)–(8)). In order to assess the contribution to P_o of a kth population of events (exponential component) of an open or a closed time distribution, it was necessary to calculate the mean open and closed times of each population ($t_{o,k}$ and $t_{c,k}$, respectively). These mean times, as well as the total mean open and closed times of the whole record (t_o and t_c, respectively), were calculated from the results of the exponential fits described above. The contribution of a population of openings to the total mean open time and thus to P_o is given by $t_{o,k}/t_o$; the same applies to closed times (eqns (8*a*) and (8*b*)). Since $t_k = a_k\tau_k$ (eqn. (4)), using the fraction of total area under the fitted curve (a_k) for estimating the contribution of a given exponential population to P_o is misleading; the scarcity of long events is compensated for by their long duration. It is also important to note that in a single exponential distribution mean time (t) equals the kinetic time constant (τ). In a multiexponential distribution, mean open or closed time of a kth exponential component (population of events) does not correspond to τ_k; actually, they may differ by orders of magnitude (compare, for example, τ_{c5} and t_{c5} in Table 1).

Figure 2*E* summarizes the contributions of the different exponential components to total open and closed times. In the open time distribution, GIRK1/5 and GIRK1/4 showed statistically significant differences: the population of events with longer τ_o (τ_{o2}) contributed more than 90% of the total open time in GIRK1/5 and less than 75% in GIRK1/4; correspondingly, the contributions of the population with shorter τ_o (τ_{o1}) showed an inverse relationship. In the closed time distributions, a noteworthy feature of both channel types was the outstanding contribution of the long closed times. The longest closures with a τ_c of about 1–2 s (τ_{c5}), which constituted only 1–3% of all closed times by area (Table 1), contributed 30% (GIRK1/5) to 55% (GIRK1/4) of total closed time (Fig. 2*E*). In GIRK1/4, this population of closures contributed a significantly larger part of total closed time than in GIRK1/5. The second longest population of closures with a τ_c of ~240 ms (τ_{c4}) contributed < 13% by area but ~33–44% by time. The short closures with a τ_c of 0·5–0·6 and 4–4·9 ms contributed less than 5%, although they were the most abundant by area.

Further examination of Table 1 reveals that the total mean open time of GIRK1/4 was ~1·9 times shorter and the total mean closed time was ~2·2 times longer ($P < 0{\cdot}05$) than those of GIRK1/5. The longer t_{o2} of GIRK1/5 is the sole factor underlying the difference in total open time; the higher value of the longest closed time, t_{c5}, of GIRK1/4 is the main reason for the longer total closed time of GIRK1/4. The differences in open and closed times explain, and contribute approximately equally to, the observed difference in P_o values of the two channels. The long closures (t_{c4} and t_{c5}) constitute 89% of the total time of GIRK1/4 activity and explain the low value of P_o.

Analysis of frequency of openings of GIRK1/4

It is important to establish that GIRK1/4 expressed in oocytes is similar to its cardiac counterpart. One way is to compare the behaviour of GIRK1/4 in the frequency domain, since a very detailed analysis of this kind has recently been performed in rat atrial myocytes (Ivanova-Nikolova *et al.* 1998). We have precisely followed the steps described in the above work. The record was divided into 400 ms segments. In each segment, we measured the frequency of opening, $f_{o,s}$ (n_s (0·4 s)$^{-1}$, where n_s is the number of openings in a segment) and the total open time within the segment, $T_{o,s}$, and calculated the open probability, $P_{o,s}$ ($T_{o,s}$ (0·4 s)$^{-1}$). Since $T_{o,s} = n_s t_{o,s}$, where $t_{o,s}$ is the mean open time in this segment,

$$t_{o,s} = P_{o,s}/f_{o,s}. \quad (9)$$

Figure 3*A* shows the frequency diagram of a 100 s portion of a record after activation by $G_{\beta\gamma}$ (out of a total of ~460 s in this cell; same patch as in Fig. 2). Similar to what has been observed in atrial cells (Ivanova-Nikolova *et al.* 1998), this diagram demonstrates the presence of 400 ms segments with a large number of openings (high frequency of opening), probably reflecting the occurrence of bursts of openings, interspersed with segments of low frequency of opening. A similar pattern was observed during the whole time of recording in this patch and in the other three patches tested. To improve the accuracy and resolution of the further analysis, the data from all four patches were combined into one distribution (total recording time, 27 min). The fraction of 'null' segments (with no openings) was 0·48.

The frequency histogram was best fitted with three geometricals with characteristic frequencies of 0·6, 4 and 34·5 Hz (Fig. 3*B*); fitting with four geometricals did not give better results. Thus, like in atrial cells (Ivanova-Nikolova *et al.* 1998), at least three populations of 400 ms segments with different frequency characteristics can be detected after activation by $G_{\beta\gamma}$.

Next, we analysed the distribution of open times within the 400 ms segments. Figure 3*C* shows an all-points presentation of this distribution. Interestingly, the segments with the lowest f_o (i.e. those that showed one or a few openings per 400 ms) showed a wide range of open times, instead of having the shortest t_o as would be expected if they represented the activity of the channel with the lowest number of bound $G_{\beta\gamma}$ and poorest opening (Ivanova-Nikolova *et al.* 1998). Figure 3*D* shows that the averaged $t_{o,s}$ values in the different frequency classes were quite similar along the whole range of frequencies. Importantly, these data are practically identical to those obtained by Ivanova-

Nikolova *et al.* (1998) after activation of cardiac GIRK with $G_{\beta1\gamma5}$, strongly supporting the relevance of studying GIRK1/4 in oocytes. The mean t_o was 1·77 ± 0·10 ms (1920 segments), very close to the value of 1·86 ± 0·09 ms obtained by Ivanova-Nikolova *et al.* (1998) with $G_{\beta1\gamma5}$ (and also similar to 1·98 ± 0·32 ms calculated from the kinetic analysis; Table 1).

Slow modal gating of GIRK1/4

From visual examination of our records it was apparent that the channel 'cycles' between periods of many seconds with bursting activity, and even longer periods dominated by single openings, long closures and scarce, short bursts. This is exemplified in Fig. 4 which shows a 320 s stretch of record from the same patch as in Figs 2 and 3*A*. This behaviour is a sign of modal gating, as found in voltage-dependent Ca^{2+} and Na^+ channels (Delcour & Tsien, 1993; Keynes, 1994).

P_o diaries with 0·4, 2 or 5 s bins (Fig. 5*A*; 2 s bins) supported the impression that the channel cycles between long periods of a 'burst' mode of openings and a 'low-P_o' mode. The 2 s bin data were chosen to select periods of the record (clusters, or runs) with either low or high P_o, with the average P_o of the whole record as the cut-off P_o (null segments were included). The $|Z|$ values were calculated as described by Colquhoun & Sakmann (1985) for each record and were in the range 5·8–7·3. Such values of $|Z|$ suggest that segments with similar P_o are unlikely to be randomly distributed and thus segments with similar P_o probably cluster together. Although the runs analysis is a relatively crude indicator of modal gating (Colquhoun & Sakmann,

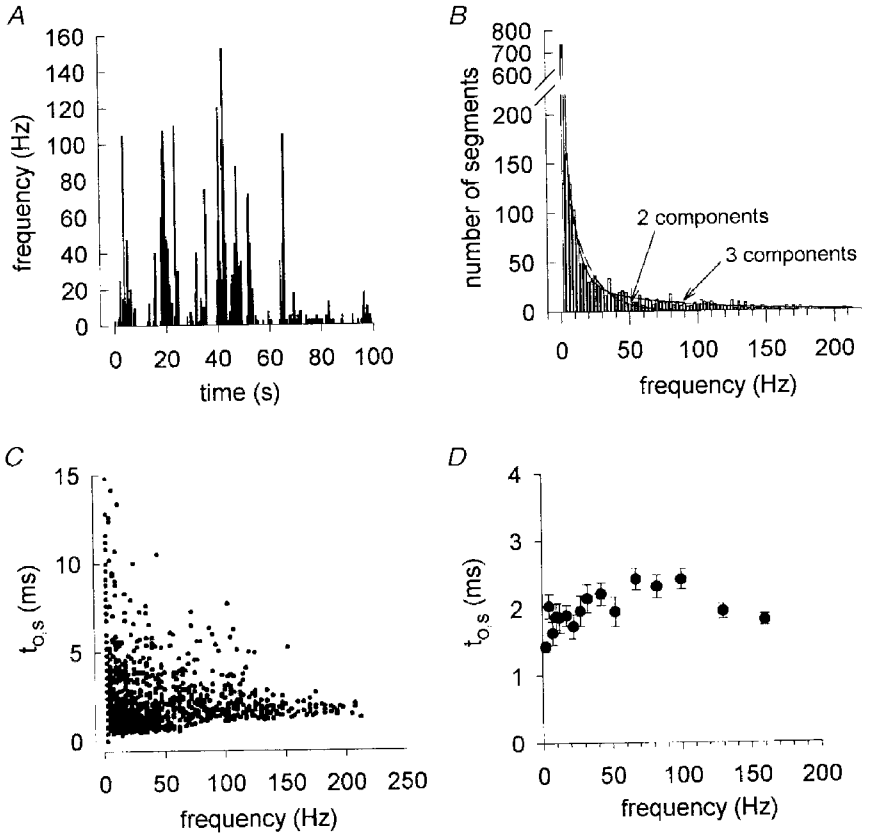

Figure 3. Frequency analysis of single-channel behaviour of GIRK1/4

The recordings were divided into consecutive 400 ms (2·5 Hz) segments, and P_o and frequency of opening were calculated for each segment. *A*, open frequency of a 100 s long stretch of record from the patch shown in Figs 2*A* and 4. *B–D*, results of analysis of data pooled from all four patches. Within the range 2·5–12·5 Hz, data were averaged for each segment separately. In the 15–35 Hz range, data from two segments were pooled; in the higher ranges, data from more segments were pooled into the following classes (in Hz): 37·5–45, 47·5–57·5, 60–75, 77·5–90, 92·5–115, 117·5–140, > 140. *B*, histogram of frequencies of channel openings. Data were fitted to the sum of two or three geometricals, $F = \Sigma n_k \mu_k^{-1}(1 - 1/\mu_k)^{f-1}$, where F is the number of observations per bin, n_k is the total number of segments contributed by a given population within the distribution, f is frequency and μ_k is the characteristic frequency of a given population. The characteristic frequencies of opening obtained by these procedures were: with two-exponential fit, $\mu_1 = 1{\cdot}5$ Hz, $\mu_2 = 16{\cdot}3$ Hz; with three-exponential fit, $\mu_1 = 1{\cdot}1$ Hz, $\mu_2 = 7{\cdot}7$ Hz, $\mu_3 = 68{\cdot}6$ Hz. *C*, scatter diagram of $t_{o,s}$ *vs.* open frequency. Each data point represents $t_{o,s}$ calculated in an individual segment and plotted against the frequency of opening measured in the same segment. *D*, t_o does not significantly change with an increase in the frequency of opening.

1985), it further supports the assumption of modal behaviour of GIRK1/4 at a constant concentration of $G_{\beta\gamma}$ on the long time scale.

For further analysis, clusters of segments with P_o above the cut-off level were designated as belonging to the burst mode and the rest were classified as belonging to the low-P_o mode; separate event lists were made for each cluster. The process of selection is illustrated in Figs 4 and 5*A*, where the boundaries of burst/low-P_o clusters are indicated by triangles. Some periods of the record were omitted because they were of low quality or for simplicity (e.g. relatively short burst or low-P_o periods, usually less than 10 s, making the analysis very tedious). An example is the stretch between ~310 and ~365 s in the record of Fig. 5*A* (indicated by a dashed line between two triangles). The mean durations of the clusters were $19{\cdot}8 \pm 3{\cdot}9$ s ($n = 15$) in the burst mode and $46{\cdot}8 \pm 7{\cdot}6$ s ($n = 16$) in the low-P_o mode. In all, data from ~70% of the total recording time were processed; this contained 77·3% of all openings. Data from burst mode clusters and from low-P_o mode clusters from all four patches were combined, forming two sets of data that were analysed separately. The overall P_o in the two sets of data was 0·102 in burst mode and 0·0034 in low-P_o mode (Fig. 6*C*).

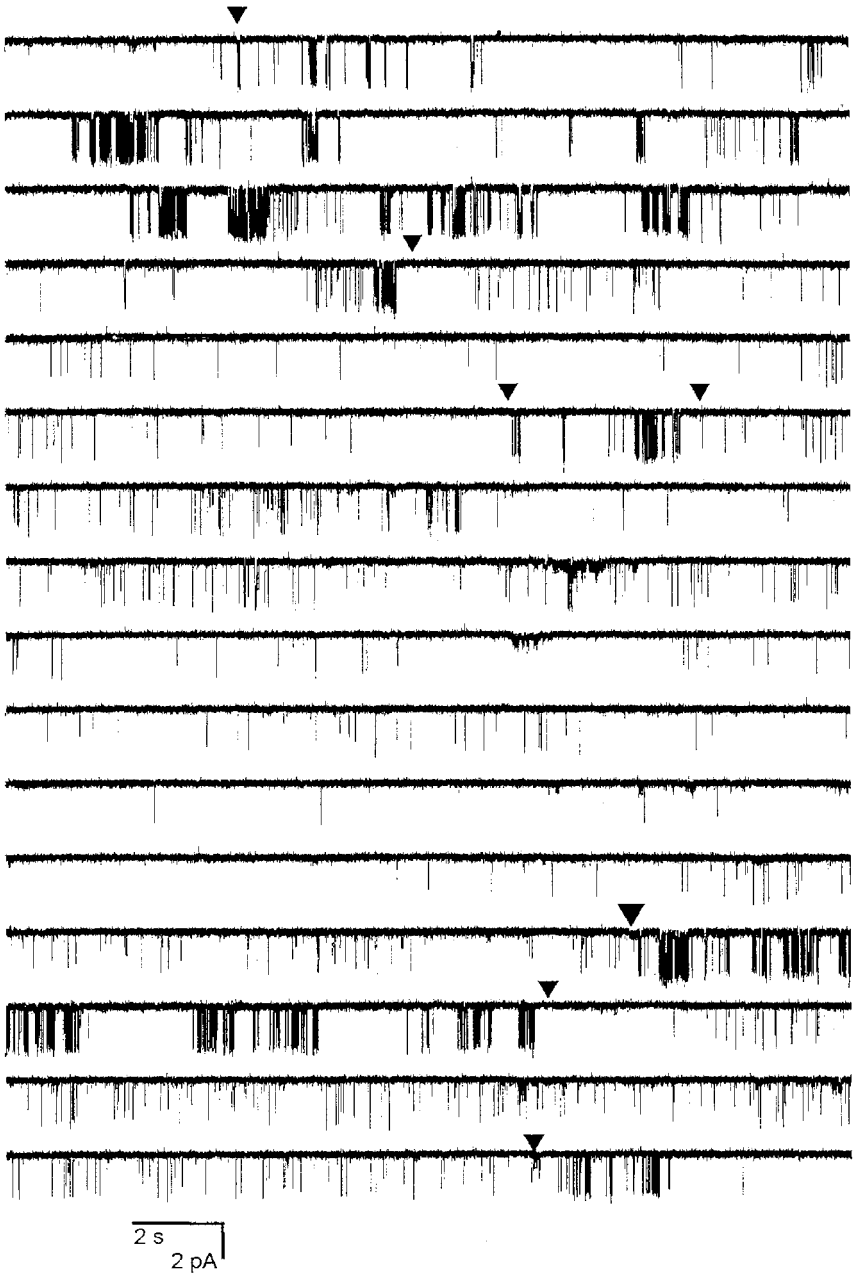

Figure 4. GIRK1/4 activated by $G_{\beta\gamma}$ 'cycles' between periods of low and high P_o
A 320 s segment of the record of GIRK1/4 activity after activation by 20 nM $G_{\beta\gamma}$. The inverted triangles show the boundaries between clusters of burst and low-P_o modes, as in Fig. 5*A*.

Frequency analysis with 400 ms segments, as performed previously for the whole record, revealed striking differences between burst and low-P_o modes. Two-hundred out of 712 segments in the burst mode (28%), and 1244 out of 2130 segments in the low-P_o mode (58%) were empty, that is, contained no openings. The mean open times of the two sets of data were clearly different across the whole frequency range (Fig. 5*B*). In low-P_o mode, $t_{o,s}$ was always 2–3 times lower than in the corresponding frequency class of the burst mode; in most frequency classes, the difference was statistically significant. Note especially the lowest frequency class, 2·5 Hz (one opening per 400 ms segment), which is supposed to be the lowest t_o class in the model of Ivanova-Nikolova *et al.* (1998). It existed in both burst and low-P_o modes though was more abundant in the low-P_o mode, but the mean $t_{o,s}$ differed greatly: 3·41 ± 0·58 ms (64 segments) *vs.* 1·14 ± 0·06 ms (468 segments, $P < 0{\cdot}001$) for burst and low-P_o mode, respectively. The average overall t_o was 2·74 ± 0·11 ms (502 segments) in the burst mode, and 1·24 ± 0·04 ms (886 segments) in the low-P_o mode; the 2·2-fold difference was highly significant ($P < 0{\cdot}001$). Most of the open time was contributed by the burst mode: 79% of all openings appeared within the periods of burst mode, and only 21% appeared in low-P_o mode. Thus, low-P_o and burst mode were characterized by different t_o values, which is usually considered an indication of different modalities of gating (Delcour *et al.* 1993). The histograms of frequency of opening were also remarkably different between the two modes (Fig. 5*C* and *D*). In both cases, the frequency distributions could be fitted with two geometricals;

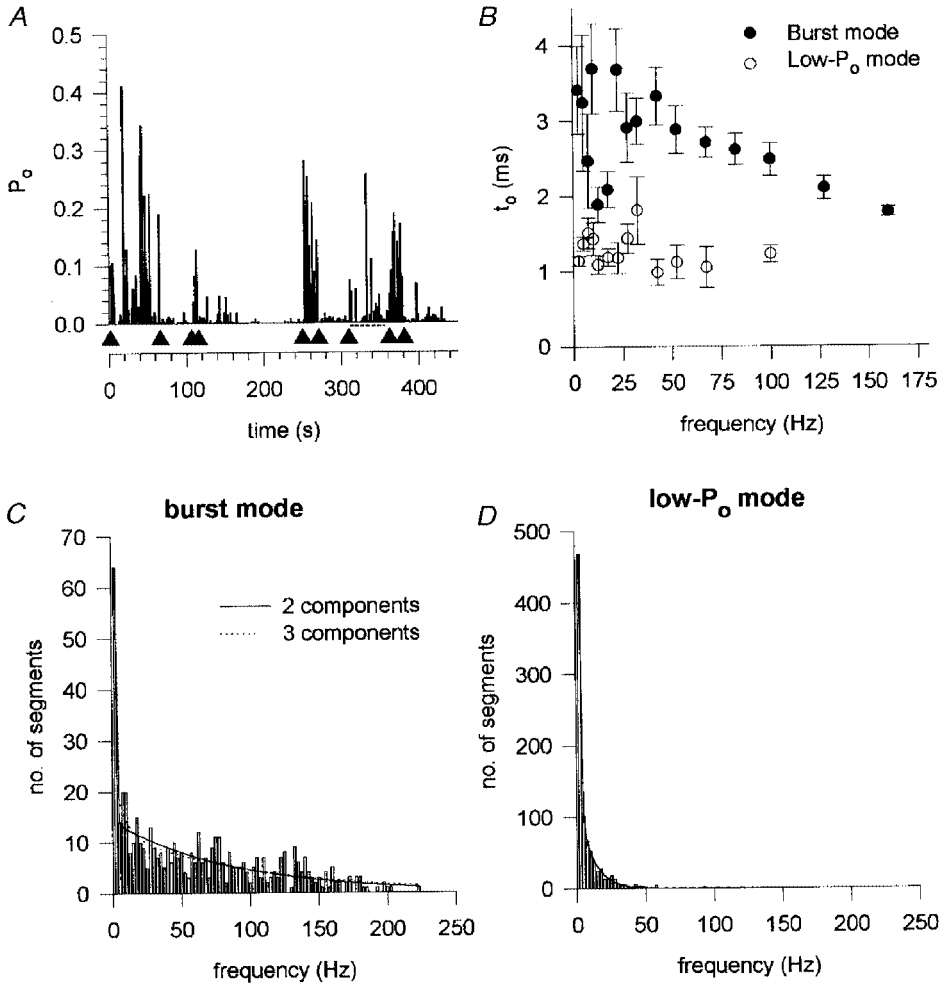

Figure 5. Frequency analysis of GIRK1/4 behaviour within low-P_o and burst modes

A, P_o diary of a representative record; same patch as in Figs 2, 3*A* and 4. *B*, the relationship between mean open time and frequency of openings within low-P_o and burst modes. Subdivision into frequency classes was done as explained in Fig. 3. *C* and *D*, histograms of frequencies of channel openings in burst and low-P_o modes, respectively. Data were fitted as in Fig. 3*B*. In the burst mode, the characteristic frequencies were: with two geometricals, 1·24 and 88·6 Hz; with three geometricals, 1·16, 7·9 and 104·3 Hz. The 'additional' 7·9 Hz population accounted for only 2·6% by area. In low-P_o mode, the characteristic frequencies were 1·46 and 10·7 ms. Fitting with three geometricals was also performed (not shown). In both modes, fits with two geometricals gave satisfactory results, and the quality of the fit was not improved by assuming three geometricals.

assuming three geometricals did not improve the fit. The two modes shared only the low frequency population with a characteristic frequency of 1·24–1·46 Hz. Each of the modes had only one additional frequency population: the burst mode had a characteristic frequency of 88·6 Hz, and the low-P_o mode had a characteristic frequency of 10·7 Hz.

In order to further characterize the differences between the two modes of gating we performed a full kinetic analysis of the high-P_o and low-P_o sets of data. The results are summarized in Fig. 6 and in Table 1. A visual examination of the open and closed time histograms shown in Fig. 6*A* and *B* reveals significant differences between burst and low-P_o modes (the use of probability density plots, which show normalized frequencies of openings and closures, enables direct comparison of the different sets of data). Open time histograms (Fig. 6*A*) revealed a relative abundance of shorter openings in the low-P_o mode (grey bars) compared to the burst mode (open bars). The open time distributions within each mode could not be satisfactorily fitted to a single-exponential function (not shown), and two exponentials were required in both cases (shown in Fig. 6*A*). Both open time constants, especially the shorter one, were substantially smaller in the low-P_o mode than in the burst mode (Table 1). These results suggested that the total open time distribution, without separation into modes (Fig. 2), probably contained more than two exponential components despite the reasonable fit obtained with the two-exponential function. The mean open time was more than 2 times greater in the

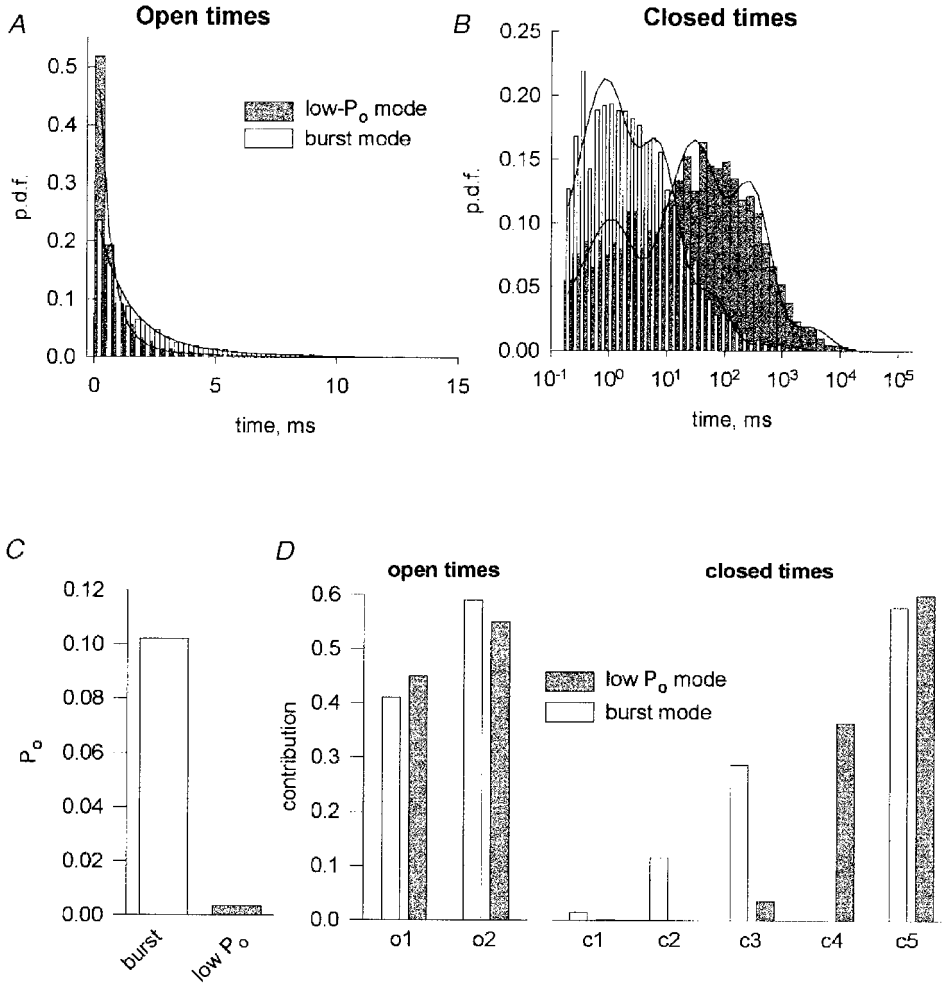

Figure 6. Kinetic analysis of GIRK1/4 gating within burst and low-P_o modes

Data were pooled from four patches before the analysis. *A*, open time distributions (in the p.d.f. form) corresponding to burst and low-P_o modes, shown superimposed. The continuous lines show the corresponding two-exponential fits. The parameters of the fit are shown in Table 1. *B*, closed time distributions (with logarithmic time bins) corresponding to burst and low-P_o modes, shown superimposed. For presentation purposes only, the first two bins were subdivided into smaller ones, and the numbers of events in each bin were interpolated. The curves show the results of the standard fitting procedure to linear p.d.f. histograms (as explained in Figs 1*C* and 2*C*) with four exponents. The parameters of the fit are shown in Table 1. *C*, open probabilities in the two modes. *D*, contribution of the exponential components of distributions of open and closed times to total open and closed times in burst and low-P_o modes.

burst than in the low-P_o mode (Table 1); however, this difference alone could not explain the 30-fold higher P_o of the burst mode.

The differences between closed time distributions were even more striking (Fig. 6*B*); long closed times were obviously much more abundant in the low-P_o mode (grey bars) than in the burst mode (open bars). Four exponential components were detected in both burst and low-P_o modes (Fig. 6*B*; Table 1). The use of five exponents did not improve the quality or the stability of the fit in either case. Furthermore, some of the characteristic time constants obtained in the four-exponential fits within modes showed striking similarities to the five closed time constants of the total distribution (Table 1). The shortest, τ_{c1}, was very similar in the total distribution of GIRK1/4 patches and in the two modes, being 0·6–0·9 ms. τ_{c2} (~5 ms) of the total distribution was boldly represented in the burst mode but absent from the low-P_o mode. The next time constant, of 23 and 46 ms for the burst and low-P_o mode, respectively, probably corresponds to τ_{c3} of the total distribution (31 ms). The next population of closures, characterized by a τ_{c4} of 240 ms, was undoubtedly contributed exclusively by a major subpopulation which is present in the low-P_o mode ($\tau = 238{\cdot}5$ ms), but absent from the burst mode. Finally, the longest time constant, τ_{c5}, appeared smaller in the burst mode (760 ms) than in the total population or in the low-P_o mode; however, the estimate of this time constant was not very accurate because of the relative rarity of the long closures in the burst mode.

The total mean closed time in the low-P_o mode was more than 10-fold greater than in the burst mode (Table 1), suggesting that the great difference in the P_o was mainly due to this factor. Analysis of the contributions of the components of the exponential distributions in the two modes (Fig. 6*D*) showed that the populations with short and long open times contributed approximately equally to the total open time. Again, the differences between the modes in the closed times are remarkable. In the low-P_o mode, the short closures are unimportant, and the two populations with the longest τ, τ_{c4} and τ_{c5} (~240 and ~2700 ms) account for > 95 % of the total closed time. In contrast, in the burst mode two out of the three shorter classes of closures (τ_{c2} and τ_{c3}; ~6 and 47 ms) make a substantial contribution (> 40 %) to the total closed time.

Modal behaviour of the GIRK1/5 channels

From visual inspection of the records and P_o data (2 s segments) it appeared that modal behaviour is much less obvious in GIRK1/5 than in GIRK1/4 channels. However, runs analysis rendered $|Z|$ values in the range 4–8·4, suggesting that clustering of segments with similar P_o is unlikely to happen by chance. A more detailed analysis was therefore performed as for GIRK1/4 channels (to avoid the ambiguity of different sampling frequencies, 5 cells with a sampling frequency of 2·5 kHz were selected for the present analysis). Mean t_o values corresponding to the two presumptive modes were significantly different (4·37 ± 0·16 ms for burst mode and 2·73 ± 0·07 ms for low-P_o mode, $P < 0{\cdot}001$). The overall P_o values in burst and low-P_o mode were 0·122 and 0·029, respectively. Note that this ~4-fold difference in mean P_o was much smaller than in GIRK1/4 channels (~30-fold).

Frequency analysis did not show explicit differences between modes in the same way as for GIRK1/4 channels. Both burst mode and low-P_o mode frequency distributions could be well fitted with two geometricals which gave rather close values of characteristic frequencies (1·16 and 38·03 Hz for the burst mode, 1·09 and 18·66 Hz for the low-P_o mode). Similarly, kinetic analysis of the high- and low-P_o sets of data did not give as clear a picture as in the case of GIRK1/4. Open time distributions in both modes were satisfactorily fitted with two exponents, of which only the longer one appeared to diverge substantially between the modes (1·06 and 6·28 ms for the burst mode, 0·85 and 3·52 ms for the low-P_o mode). According to closed time distribution analysis, it appeared that the low-P_o mode probably contained all five closed time components that were found in the whole records. The burst mode closed time distribution could be fitted with four exponents, omitting the long exponent found in the low-P_o mode.

GIRK1/4 gating after inhibition by $G_{\alpha i1}$

GIRK1/5 channels are inhibited by GTPγS-activated, myristoylated $G_{\alpha i1}$ with an IC_{50} close to 15 pM; at 100 pM, the inhibition reaches 95 % (Schreibmayer *et al.* 1996). This inhibition is not due to sequestration of $G_{\beta\gamma}$ but to another, unknown mechanism. In rat atrial myocytes, inhibition was ~85 %, apparently less than that of GIRK1/5 (Schreibmayer *et al.* 1996). Although in the same work we also observed inhibition of GIRK1/4 channels expressed in the oocytes, neither channel kinetics nor the mechanism of inhibition by $G_{\alpha i1}$ was analysed in detail. The pattern of channel activity in the presence of $G_{\alpha i1}$ was characterized by long shut periods and low P_o, resembling the low-P_o mode and raising the possibility that $G_{\alpha i1}$ may be one of the cellular factors controlling the modal behaviour of GIRK. Therefore, we decided to make a detailed analysis of $G_{\alpha i1}$-induced inhibition of GIRK1/4.

The excised patches were exposed to 20 nM $G_{\beta\gamma}$ alone or together with 25 or 100 pM $G_{\alpha i1}$. As can be seen from Fig. 7*A*, in many patches the inhibitory effect of $G_{\alpha i1}$ could be easily seen. However, in most cases a substantial activation of GIRK1/4 was still observed in the presence of $G_{\alpha i1}$. To quantify the effects of $G_{\beta\gamma}$ and $G_{\alpha i1}$, the extent of activation by $G_{\beta\gamma}$ in each patch was normalized to the basal activity in the same patch, by calculating NP_o in the presence of $G_{\beta\gamma}$ divided by basal NP_o. NP_o in the presence of $G_{\beta\gamma}$ was measured during a 1 min period of maximal activity, between 2 and 7 min after addition of $G_{\beta\gamma}$. Basal NP_o was measured during the second minute after patch excision.

The estimation of NP_o in patches with very low basal activity (less than 3–4 openings min^{-1}) was unreliable, therefore patches with basal $NP_o < 0{\cdot}00005$ have been excluded from the analysis (4 out of 37 patches).

A summary of these experiments is shown in Fig. 7*B*. $G_{\beta\gamma}$ alone activated the channel by > 770-fold. In the presence of GTPγS-activated $G_{\alpha i1}$ the activation was attenuated by about 70 %, but was still very substantial at ~200-fold. The inhibition could be easily overlooked if thorough comparisons with the control activation by $G_{\beta\gamma}$ were not performed in the same oocyte batches.

In four patches activated by $G_{\beta\gamma}$ in the presence of $G_{\alpha i1}$, no overlaps of openings were observed during the whole time of the record (7–10 min after $G_{\beta\gamma}$ application). Since there were relatively few openings in each of these records, data from these four patches were combined, and open and closed kinetics were analysed as previously. Open time distribution was fitted with two exponents (Fig. 7*C* and Table 1). Closed time distribution was fitted with four exponents (Fig. 7*D*), close but not identical to those of the low-P_o mode (Table 1).

Frequency analysis of GIRK1/4 gating in the presence of $G_{\alpha i1}$ rendered characteristic frequencies of 1·13 and 7·47 Hz, similar to those found in the low-P_o mode of GIRK1/4 (1·46 and 10·7 Hz).

DISCUSSION

Single-channel recordings

Full analysis of channel kinetics, including the closed states, requires recordings from patches containing one channel. Our criterion for selecting patches with one channel was the lack of overlapping openings for the whole duration of the experiment, in the presence of an almost saturating concentration of $G_{\beta\gamma}$. In the case of GIRK1/4 channels, all records contained at least 5000 events; that is, $n(o) = 2500$ openings. The approximate probability of not observing an overlap in such a record, P_r, is given by the expression $P_r = \{(1 - P_o)/(1 - P_o/N)\}^{n(o)-1}$, where N is the actual number of channels in the patch (Colquhoun & Hawkes, 1995). With $P_o = 0{\cdot}025$ for GIRK1/4 (Fig. 2), the probability of not detecting a second channel ($N = 2$) even

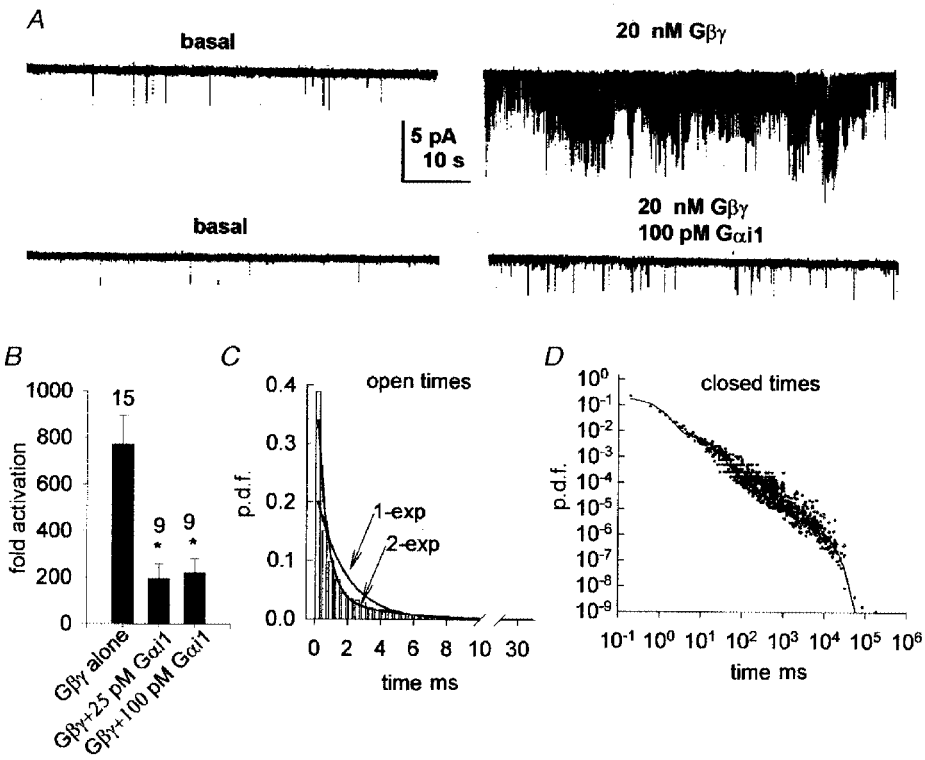

Figure 7. Inhibition of $G_{\beta\gamma}$-induced activation of GIRK1/4 by GTPγS-activated myristoylated $G_{\alpha i1}$

A, basal (left) and $G_{\beta\gamma}$-induced (right) activity in two excised patches of oocytes expressing GIRK1/4. The right-hand upper record shows activation by 20 nM $G_{\beta\gamma}$; in the right-hand lower record, $G_{\beta\gamma}$ was applied together with 100 pM GTPγS-activated, myristoylated recombinant $G_{\alpha i1}$. *B*, summary of the extent of activation by $G_{\beta\gamma}$ in the absence and presence of $G_{\alpha i1}$. Numbers above bars show the number of patches; asterisks indicate a significant difference from control ($P < 0{\cdot}05$). *C* and *D*, kinetic analysis of single GIRK1/4 channel behaviour after activation by 20 nM $G_{\beta\gamma}$ in the presence of GTPγS-activated, myristoylated $G_{\alpha i1}$. Data were pooled from four patches in which no overlaps of opening were observed after $G_{\beta\gamma}$ application. *C*, open time distribution and one- and two-exponential fits. The parameters of the fits were: for one-exponential fit, $\tau_o = 1{\cdot}764$ ms; for two-exponential fit, see Table 1. *D*, closed time distribution. Probability density plot and four-exponential fit; for parameters see Table 1.

in our shortest record is negligible ($1{\cdot}5 \times 10^{-14}$). Since the P_o of GIRK1/5 is higher than that of GIRK1/4, the probability of missing a second channel in GIRK1/5 recordings is even lower. Thus, all our records can be considered as genuine single-channel ones. On the other hand, when the channels are inhibited by $G_{\alpha i1}$, the P_o drops by ~70%, and the number of recorded openings is also much smaller. Assuming $P_o = 0{\cdot}0075$ and $n(o) = 500$, the probability of missing a second channel in such a recording is very high (0·152); the probability of missing a third channel is 0·082. Thus, some or all of our records with $G_{\alpha i1}$ which showed no overlaps of openings probably contained more than one channel, and the results of the analysis should be treated accordingly.

The accuracy of our estimates of the fastest kinetic constants was probably impaired by the relatively low acquisition rates used (0·25–0·4 ms per point), despite the correction for missing events. However, the error may not be too significant, because the estimates of the open time constants fit quite well with those reported by others in atrial cells (see below), where recordings were made with higher acquisition rates.

A more serious problem could be that missing very short openings within long closed intervals would lead to an overestimation of the long closed times. Such reservation, however, must be applied to kinetic analysis of any single-channel record, taken at any recording frequency, because the lowest limit to the duration of a single opening may be in the nanosecond range, which is the time scale of movement of single amino acids in the proteins (Hille, 1992*b*). Capturing such openings would be impossible with the existing recording methods. Therefore, the closed time constants found in a kinetic analysis actually represent 'silent' periods with extremely low P_o, rather than fully non-conducting (shut) states. The presence of such missed short openings will not affect the main conclusions of this study; namely, that the GIRK channel exhibits very slow modal transitions at saturating levels of $G_{\beta\gamma}$, and that it spends most of its time in long periods of 'silence' when the channel does not conduct any significant amount of current. Throughout this paper we call such silent periods 'closures' while keeping in mind the above reservations.

Comparison of GIRK1/5 and GIRK1/4 expressed in oocytes, and atrial K_{ACh}

Although we cannot fully rule out the possibility that the endogenous GIRK5 could contribute to the formation of functional channels when both GIRK1 and GIRK4 RNA were injected into the oocytes, this seems unlikely for the following reasons. (i) The low concentrations of GIRK1 RNA used in the study of GIRK1/4 ensured that the density of GIRK1/5 channels would be extremely low; when such amounts of GIRK1 RNA were injected alone, we failed to 'catch' expressed channels with standard pipettes. (ii) The expressed GIRK1/4 channels were clearly distinct from GIRK1/5 channels in the 3-fold lower P_o (Fig. 2) and the different values of several kinetic parameters (τ_{o2}, a_{c2}, t_{c5}, total closed time; see Table 1). We conclude that, in oocytes injected with GIRK1 and GIRK4 RNA, the recorded activity belonged to genuine GIRK1/4 channels, with little or no interference from GIRK5.

The properties of the expressed GIRK1/4 are very similar to those of $G_{\beta\gamma}$-activated atrial K_{ACh}, as shown by a number of parameters. One set of parameters comes from the analysis of frequencies of opening (Fig. 3). As for the expressed GIRK1/4 channel described here, in atrial myocytes the distribution of frequencies of opening of $G_{\beta\gamma}$-activated K_{ACh} was fitted by three geometricals (Ivanova-Nikolova *et al.* 1998). Mean open time was almost identical to that in atrium (1·77 and 1·86 ms, respectively) and did not change as a function of frequency of opening. These data also support the view that combinations of $G_{\beta 1}$ with different G_γ subunits ($G_{\gamma 2}$ in our case, $G_{\gamma 5}$ in the experiments of Ivanova-Nikolova *et al.* 1998) activate the channel in a similar way and with a similar potency (Wickman *et al.* 1994).

The kinetic parameters of the open time distribution of K_{ACh} and the expressed GIRK1/4 are also similar. In mammalian atrial GIRK, in the presence of ATP there are at least two open states, with time constants of ~1–1·4 and 4–7 ms (Kim, 1991; Nemec *et al.* 1999). These values are somewhat higher than those that we found in the analyses of total GIRK1/4 records (Table 1). However, it is notable that, in atrial cells, the analyses were usually done on multi-channel patches or only within bursts. Since P_o in the burst mode is ~30-fold higher than in the low-P_o mode, in any selected stretch of a multichannel record the low-P_o mode will be under-represented if at least one of the channels is gating in the burst mode. Therefore, it is sensible to compare the open time constants reported in the literature with those of the burst mode found here (1·24 and 4·07 ms); in this case the agreement is very good.

The comparison of closed times is practically impossible because of the scarcity of data and differences in preparation and recording conditions. In rat and frog atria, closed times of ACh-activated channels of 0·2–80 ms have been reported (Sakmann *et al.* 1983; Ivanova-Nikolova & Breitwieser, 1997). The reason for not detecting the very long closures observed here could be the different focus of these reports (mainly on short gating transitions and bursts), the use of patches with more than one channel, or the fact that in some cases mainly periods of bursting were analysed (e.g. Ivanova-Nikolova & Breitwieser, 1997). The long closures of hundreds of milliseconds (τ_{c4} and τ_{c5}) observed here contributed > 90% to the total time the channel spent in states where no openings were detected. It is this high contribution of long 'silent' periods that is responsible for the low P_o of GIRK1/4; the fast closures are quite unimportant in determining the total closed time and P_o. The overall very low P_o, the presence of the long closures and their importance in determining the P_o (and thus the macroscopic parameters of channel activity) were not previously appreciated.

Modal transitions on the slow time scale

Our results demonstrate that $G_{\beta\gamma}$-activated GIRK1/4 channels display a clear modal gating over a long time scale. This is apparent from a visual examination of the records and is supported by several types of analysis. First, runs analysis showed that clustering of 2 s segments with similar P_o is highly unlikely to happen by chance. Second, as deduced from P_o diaries, channel behaviour periodically shifts (cycles) from a bursting, high-P_o pattern to a low-P_o pattern dominated by short bursts and single openings. The difference in P_o between the two modes was 30-fold. Such slow cycling strikingly resembles the modal gating of voltage-dependent Ca^{2+}, Cl^- and Na^+ channels, and Ca^{2+}-dependent K^+ channels (Hess *et al.* 1984; Blatz & Magleby, 1986; Zhou *et al.* 1991; Delcour & Tsien, 1993; Imredy & Yue, 1994; Keynes, 1994; Smith & Ashford, 1998), but it has never before been described for GIRK channels. Third, the sets of kinetic time constants of open and closed states in the two modes showed substantial differences. Fourth, the distributions of frequencies of openings, as well as mean open time values, were significantly different in the two modes. These features, too, are important indicators of modal gating (e.g. Delcour & Tsien, 1993).

Open times were best fitted assuming a two-exponential distribution in both burst and low-P_o modes. Both τ_{o1} and τ_{o2} differed between the two modes. The different τ_o values cannot be compared statistically, since the analysis in this case was done on pooled data. However, the independent frequency analysis (Fig. 5) strongly supports this conclusion. It showed a highly significant difference in the duration of single openings within the two modes: the mean open time in the lowest frequency class of 2·5 Hz, i.e. where a *single opening* occurs within a 400 ms segment, was 3-fold lower in the low-P_o mode than in the burst mode. The fast open kinetics of GIRK channels and of the other members of the inwardly rectifying K^+ channel, K_{ir}, superfamily is believed to be determined by the properties of the pore (Reuveny *et al.* 1996; Chan *et al.* 1996*b*). For instance, bursting behaviour can be conferred on homomultimeric GIRK4 channels by mutation of a single residue, S143, within the presumptive pore region (Chan *et al.* 1996*b*; Vivaudou *et al.* 1997). Thus, it is probable that transitions between the modes correlate with rearrangements within the pore.

The closed kinetics were very complex in both modes; our fitting procedures indicated that each closed time distribution was composed of up to four exponential components. τ_{c1}, τ_{c3} and τ_{c5} were similar between the two modes, and it is also possible that they actually represented the same kinetic populations (Table 1). Thus, on the molecular level, some of the processes leading to channel closure appear to be unchanged by the mode switch. On the other hand, the burst mode also contained a prominent population of closures with a τ_c of ~6 ms (τ_{c2}) which was not detected at all in the low-P_o mode; this might represent closures within long bursts which are absent in the low-P_o mode. Similarly, a very prominent population of closures in the low-P_o mode with a τ_c of ~240 ms (τ_{c4}), also easily detected in the analysis of the whole record before subdivision into modes, was practically absent from the burst mode. Thus, the two modes are characterized by different sets of kinetic constants.

Interestingly, slow modal transitions (if they existed) were much less obvious in GIRK1/5 channels. No clear-cut subdivision into kinetically distinct modes could be performed in the same way as for GIRK1/4. Although it cannot be concluded with certainty that such modes do not exist in GIRK1/5, the lack of clear slow modal behaviour in these channels as compared with GIRK1/4 emphasizes the role of the GIRK4 subunit in generating this type of gating.

Is slow modal behaviour driven by binding and unbinding of $G_{\beta\gamma}$?

The average durations of ~20 and ~47 s spent by GIRK1/4 in burst and low-P_o mode, respectively, indicate that very slow transitions are involved; it is hard to imagine that they are driven by $G_{\beta\gamma}$ binding and unbinding. Both measured and calculated affinities of $G_{\beta\gamma}$ for GIRK channels are in the range 2–10 nM (Wickman *et al.* 1994; Schreibmayer *et al.* 1996; Luchian *et al.* 1997; Ivanova-Nikolova *et al.* 1998). It is very unlikely that the binding constant of such a high-affinity activator would lie in the range of many seconds. Indeed, the on-rate of activation of GIRK channels by agonists (which in turn activates the receptor, then G protein, and then $G_{\beta\gamma}$ is released and binds to the channel) is less than half a second, suggesting binding of $G_{\beta\gamma}$ within much less than a second (for review, see Hille, 1992*a*).

Ivanova-Nikolova *et al.* (1998) reported modal changes in the gating of K_{ACh} channels in cell-attached patches in rat atrium upon activation by ACh. The two main observations were: (i) the distribution of frequencies of openings showed four geometrical components, with higher frequencies being promoted by higher concentrations of ACh; (ii) the mean open time of ACh-activated channels correlated with the frequency of opening and showed four distinct levels, with the highest t_o promoted by higher agonist concentrations. A model was proposed in which the channel switches between four modes of gating, in addition to the inactive basal state with no $G_{\beta\gamma}$ bound (Ivanova-Nikolova *et al.* 1998). Switches from low-frequency, low-P_o modes, to modes with higher frequency and P_o result from sequential binding of more and more $G_{\beta\gamma}$ molecules (up to four). The same work also revealed discrepancies between ACh- and $G_{\beta\gamma}$-induced activation of the channel: (i) with $G_{\beta\gamma}$ as the channel activator in excised patches, only three components of the distribution of frequencies of opening were normally observed; (ii) t_o was unchanged with increasing $G_{\beta\gamma}$ concentrations and, correspondingly, frequency of openings. As noted above, both observations are fully supported by our data; they are not compatible with the above model in its original form. Although hypothetical explanations have been offered, the actual reason for the observed discrepancies between ACh- and $G_{\beta\gamma}$-induced activity remains unknown (Ivanova-

Nikolova *et al.* 1998) and it is unclear whether the above model can be applied to $G_{\beta\gamma}$-induced GIRK activity.

Importantly, it is evident that the slow modal transitions between low-P_o and burst mode described here cannot be described by the model of Ivanova-Nikolova *et al.* (1998). This conclusion is based on the differences between ACh- and $G_{\beta\gamma}$-induced activation of GIRK1/4 mentioned above, and on two additional lines of evidence as follows.

Firstly, since the distribution of frequencies of opening in low-P_o mode has two components, then, according to the model of Ivanova-Nikolova *et al.* (1998), it should reflect the channel state with zero, one and two $G_{\beta\gamma}$ molecules bound. If it is the binding of one or two additional $G_{\beta\gamma}$ molecule(s) that drives the channel from the low-P_o mode into the burst mode, this distribution must show an additional geometrical component, and possibly should even lose the shortest one. However, this was not the case. Strikingly, in the burst mode the distribution of frequencies of opening does acquire a high-frequency component, but completely loses the intermediate one, whereas the shortest one is preserved (Fig. 5). The three-component distribution of frequencies of opening obtained from the analysis of the whole record is most probably an algebraic mixture of the two different distributions found upon separate analysis of burst and low-P_o periods.

Secondly, the frequency analysis showed an overwhelming number of long closed 400 ms segments. Ivanova-Nikolova *et al.* (1998) calculated that the maximal probability of $G_{\beta\gamma}$ binding, P_{max}, is about 0·63. The probability of $G_{\beta\gamma}$ binding at the concentration of 20 nM used in our work, which is about 10 times the K_d, should be close to P_{max} (see eqn (2) in Ivanova-Nikolova *et al.* 1998). According to binomial distribution, at almost-saturating $G_{\beta\gamma}$ concentrations, the probability of finding the channel without any $G_{\beta\gamma}$ bound ('gating mode 0') is close to $(1 - P_{max})^4 = 0{\cdot}019$. However, the proportion of null 400 ms segments in our experiments was 0·48, in disagreement with the above theory. The results presented here actually suggest that the binomial model cannot describe the behaviour of GIRK channels activated by $G_{\beta\gamma}$, and that additional possibilities must be considered (e.g. that the binding of $G_{\beta\gamma}$ to GIRK subunits is not independent).

All the above arguments strongly support the contention that the slow modal gating of GIRK1/4 described here is not driven by $G_{\beta\gamma}$ binding/unbinding. Instead, we propose the hypothesis that the gating of GIRK1/4 channels, either after or independently of $G_{\beta\gamma}$ binding, occurs in two distinct modes; the transitions between the two modes reflect slow conformational changes intrinsic to the channels, or driven by chemical reactions or by interaction with other proteins. We measured the channel activity in near-physiological experimental conditions (patches were excised into a solution containing Na^+, ATP and Mg^{2+}) designed to prevent rundown or irreversible dephosphorylation of membrane proteins or phospholipids. Therefore, the involvement of important gating factors such as phosphorylation and dephosphorylation, Na^+, or membrane phospholipids (PIP_2; see Sui *et al.* 1996, 1998) in modal gating is a valid possibility. The modal transitions may also somehow be connected to the GTPase cycle of endogenous G proteins, possibly physically linked to the channel (Huang *et al.* 1995), reflecting activation and deactivation of G_α subunits; some of them, notably $G_{\alpha i1}$, may inhibit GIRK activity in their activated, GTP-bound form (Schreibmayer *et al.* 1996). In fact, GTPγS-activated $G_{\alpha i1}$ shifts GIRK1/4 to a mode of gating similar but not identical to the low-P_o mode (Table 1). Thus, the possibility that the slow modal gating of GIRK1/4 is linked to a GTPase cycle remains uncertain but not improbable.

The presence of two major modes suggests a branched model of gating (Delcour *et al.* 1993). The branching includes the transitions between modes, and probably also branching within modes. This model can be reconciled with the observations of Ivanova-Nikolova and colleagues (Ivanova-Nikolova & Breitwieser, 1997; Ivanova-Nikolova *et al.* 1998): it is possible that the relative proportions of burst and low-P_o modes may depend on the amount of bound $G_{\beta\gamma}$ molecules, or that binding of $G_{\beta\gamma}$ molecules may alter the gating within a mode (probably the burst mode). If the latter is true, agonist-driven 'submodes' within the burst mode have to be introduced, since the agonist-induced changes in GIRK gating within bursts cannot be described by a simple linear model (Ivanova-Nikolova & Breitwieser, 1997; Nemec *et al.* 1999).

Conclusions

We have performed a detailed analysis of the single-channel kinetics of the cardiac GIRK1/4 (K_{ACh}) channel, and compared it with that of the GIRK1/5 channel. The properties of $G_{\beta\gamma}$-activated rat GIRK1/4 channels expressed in *Xenopus* oocytes are similar to those found in atrial cells, making it possible to use this powerful expression system to study GIRK channel gating. Analysis of the activity of $G_{\beta\gamma}$-activated single GIRK1/5 and GIRK1/4 channels unveiled rich closed kinetics, previously unknown, and very low open probabilities ($P_o < 0{\cdot}09$ for GIRK1/5, $P_o < 0{\cdot}03$ for GIRK1/4), a fact that was not realized before. A hallmark of gating is the abundance of very long silent periods, with no detected openings, lasting hundreds of milliseconds. These long closures accounted for almost 90% of the total duration of GIRK1/4 activity even at saturating concentrations of $G_{\beta\gamma}$, and underlie the low P_o. GIRK1/4 and GIRK1/5 differ not only in P_o but also in a number of kinetic parameters and in the presence of slow modal transitions, which are much more obvious in GIRK1/4. This suggests the importance of subunit composition in determining the single-channel kinetics. On a time scale of many seconds, the GIRK1/4 channel displays a clear modal behaviour, 'cycling' between periods of bursting activity with relatively high P_o (burst mode) and even longer periods of low P_o characterized by short bursts and single openings (low-P_o mode). Each of the modes is characterized by a

specific set of kinetic constants and, therefore, reflects a different set of channel conformations. This is the first description of slow modal transitions in GIRK channels. These transitions do not appear to be driven by $G_{\beta\gamma}$ binding or unbinding and may reflect slow regulatory processes occurring after, or independently of, $G_{\beta\gamma}$ binding.

Ashford, M. L., Bond, C. T., Blair, T. A. & Adelman, J. P. (1994). Cloning and functional expression of a rat heart KATP channel. *Nature* **370**, 456–459.

Blatz, A. L. & Magleby, K. L. (1986). Quantitative description of three modes of activity of fast chloride channels from rat skeletal muscle. *Journal of Physiology* **378**, 141–174.

Bunemann, M., Brandts, B. & Pott, L. (1996). Downregulation of muscarinic M2 receptors linked to K^+ current in cultured guinea-pig atrial myocytes. *Journal of Physiology* **494**, 351–362.

Chan, K. W., Langan, M. N., Sui, J. L., Kozak, J. A., Pabon, A., Ladias, J. A. & Logothetis, D. E. (1996*a*). A recombinant inwardly rectifying potassium channel coupled to GTP-binding proteins. *Journal of General Physiology* **107**, 381–397.

Chan, K. W., Sui, J. L., Vivaudou, M. & Logothetis, D. E. (1996*b*). Control of channel activity through a unique amino acid residue of a G protein-gated inwardly rectifying K^+ channel subunit. *Proceedings of the National Academy of Sciences of the USA* **93**, 14193–14198.

Colquhoun, D. & Hawkes, A. G. (1981). On the stochastic properties of single ion channels. *Proceedings of the Royal Society of London* B **211**, 205–235.

Colquhoun, D. & Hawkes, A. G. (1995). The principles of the stochastic interpretation of ion-channel mechanisms. In *Single-Channel Recording*, ed. Sakmann, B. & Neher, E., pp. 397–482. Plenum Press, New York.

Colquhoun, D. & Sakmann, B. (1985). Fast events in single-channel currents activated by acetylcholine and its analogues at the frog muscle end-plate. *Journal of Physiology* **369**, 501–557.

Colquhoun, D. & Sigworth, F. J. (1995). Fitting and statistical analysis of single-channel records. In *Single-Channel Recording*, ed. Sakmann, B. & Neher, E., pp. 483–587. Plenum Press, New York.

Corey, S., Krapivinsky, G., Krapivinsky, L. & Clapham, D. E. (1998). Number and stoichiometry of subunits in the native atrial G-protein-gated K^+ channel, IKACh. *Journal of Biological Chemistry* **273**, 5271–5278.

Dascal, N. (1997). Signalling via the G protein-activated K^+ channels. *Cellular Signalling* **9**, 551–573.

Dascal, N. & Lotan, I. (1992). Expression of exogenous ion channels and neurotransmitter receptors in RNA-injected *Xenopus* oocytes. In *Protocols in Molecular Neurobiology*, chap. 13, ed. Longstaff, A. & Revest, P., pp. 205–225. Humana Press, Totowa, NJ, USA.

Dascal, N., Schreibmayer, W., Lim, N. F., Wang, W., Chavkin, C., DiMagno, L., Labarca, C., Kieffer, B. L., Gaveriaux-Ruff, C., Trollinger, D., Lester, H. A. & Davidson, N. (1993). Atrial G protein-activated K^+ channel: expression cloning and molecular properties. *Proceedings of the National Academy of Sciences of the USA* **90**, 10235–10239.

Delcour, A. H., Lipscombe, D. & Tsien, R. W. (1993). Multiple modes of N-type calcium channel activity distinguished by differences in gating kinetics. *Journal of Neuroscience* **13**, 181–194.

Delcour, A. H. & Tsien, R. W. (1993). Altered prevalence of gating modes in neurotransmitter inhibition of N-type calcium channels. *Science* **259**, 980–984.

Duprat, F., Lesage, F., Guillemare, E., Fink, M., Hugnot, J. P., Bigay, J., Lazdunski, M., Romey, G. & Barhanin, J. (1995). Heterologous multimeric assembly is essential for K^+ channel activity of neuronal and cardiac G-protein-activated inward rectifiers. *Biochemical and Biophysical Research Communications* **212**, 657–663.

Grigg, J. J., Kozasa, T., Nakajima, Y. & Nakajima, S. (1996). Single-channel properties of a G-protein-coupled inward rectifier potassium channel in brain neurons. *Journal of Neurophysiology* **75**, 318–328.

Hedin, K. E., Lim, N. F. & Clapham, D. E. (1996). Cloning of a *Xenopus laevis* inwardly rectifying K^+ channel subunit that permits GIRK1 expression of I_{KACh} currents in oocytes. *Neuron* **16**, 423–429.

Hess, P., Lansman, J. B. & Tsien, R. W. (1984). Different modes of Ca channel gating behaviour favoured by dihydropyridine Ca agonists and antagonists. *Nature* **311**, 538–544.

Hille, B. (1992*a*). G protein-coupled mechanisms and nervous signaling. *Neuron* **9**, 187–195.

Hille, B. (1992*b*). *Ionic Channels of Excitable Membranes*. Sinauer, Sunderland.

Huang, C. L., Feng, S. Y. & Hilgemann, D. W. (1998). Direct activation of inward rectifier potassium channels by PIP_2 and its stabilization by $G\beta\gamma$. *Nature* **391**, 803–806.

Huang, C. L., Slesinger, P. A., Casey, P. J., Jan, Y. N. & Jan, L. Y. (1995). Evidence that direct binding of $G\beta\gamma$ to the GIRK1 G protein-gated inwardly rectifying K^+ channel is important for channel activation. *Neuron* **15**, 1133–1143.

Imredy, J. P. & Yue, D. T. (1994). Mechanism of Ca^{2+}-sensitive inactivation of L-type Ca^{2+} channels. *Neuron* **12**, 1301–1318.

Inanobe, A., Ito, H., Ito, M., Hosoya, Y. & Kurachi, Y. (1995). Immunological and physical characterization of the brain G protein-gated muscarinic potassium channel. *Biochemical and Biophysical Research Communications* **217**, 1238–1244.

Iniguez-Lluhi, J. A., Simon, M. I., Robishaw, J. D. & Gilman, A. G. (1992). G protein $\beta\gamma$ subunits synthesized in Sf9 cells. Functional characterization and the significance of prenylation of γ. *Journal of Biological Chemistry* **267**, 23409–23417.

Ivanova-Nikolova, T. T. & Breitwieser, G. E. (1997). Effector contributions to $G\beta\gamma$-mediated signaling as revealed by muscarinic potassium channel gating. *Journal of General Physiology* **109**, 245–253.

Ivanova-Nikolova, T. T., Nikolov, E. N., Hansen, C. & Robishaw, J. D. (1998). Muscarinic K^+ channel in the heart. Modal regulation by G protein $\beta\gamma$ subunits. *Journal of General Physiology* **112**, 199–210.

Jan, L. Y. & Jan, Y. N. (1997). Receptor-regulated ion channels. *Current Opinion in Cell Biology* **9**, 155–160.

Keynes, R. D. (1994). Bimodal gating of the Na^+ channel. *Trends in Neurosciences* **17**, 58–61.

Kim, D. (1991). Modulation of acetylcholine-activated K^+ channel function in rat atrial cells by phosphorylation. *Journal of Physiology* **437**, 133–155.

Kim, D., Watson, M. & Indyk, V. (1997). ATP-dependent regulation of a G protein-coupled K^+ channel (GIRK1/GIRK4) expressed in oocytes. *American Journal of Physiology* **272**, H195–206.

Kirsch, G. E. & Brown, A. M. (1989). Trypsin activation of atrial muscarinic K^+ channels. *American Journal of Physiology* **257**, H334–338.

Kofuji, P., Davidson, N. & Lester, H. A. (1995). Evidence that neuronal G-protein-gated inwardly rectifying K^+ channels are activated by $G\beta\gamma$ subunits and function as heteromultimers. *Proceedings of the National Academy of Sciences of the USA* **92**, 6542–6546.

Kozasa, T. & Gilman, A. G. (1995). Purification of recombinant G proteins from Sf9 cells by hexahistidine tagging of associated subunits. Characterization of α_{12} and inhibition of adenylyl cyclase by α_z. *Journal of Biological Chemistry* **270**, 1734–1741.

Krapivinsky, G., Gordon, E. A., Wickman, K., Velimirovic, B., Krapivinsky, L. & Clapham, D. E. (1995). The G-protein-gated atrial K^+ channel I_{KACh} is a heteromultimer of two inwardly rectifying K^+-channel proteins. *Nature* **374**, 135–141.

Kubo, Y., Reuveny, E., Slesinger, P. A., Jan, Y. N. & Jan, L. Y. (1993). Primary structure and functional expression of a rat G-protein-coupled muscarinic potassium channel. *Nature* **364**, 802–806.

Kurachi, Y. (1995). G protein regulation of cardiac muscarinic potassium channel. *American Journal of Physiology* **269**, C821–830.

Lesage, F., Duprat, F., Fink, M., Guillemare, E., Coppola, T., Lazdunski, M. & Hugnot, J. P. (1994). Cloning provides evidence for a family of inward rectifier and G-protein coupled K^+ channels in the brain. *FEBS Letters* **353**, 37–42.

Lesage, F., Guillemare, E., Fink, M., Duprat, F., Heurteaux, C., Fosset, M., Romey, G., Barhanin, J. & Lazdunski, M. (1995). Molecular properties of neuronal G-protein-activated inwardly rectifying K^+ channels. *Journal of Biological Chemistry* **270**, 28660–28667.

Liao, Y. J., Jan, Y. N. & Jan, L. Y. (1996). Heteromultimerization of G-protein-gated inwardly rectifying K^+ channel proteins GIRK1 and GIRK2 and their altered expression in weaver brain. *Journal of Neuroscience* **16**, 7137–7150.

Linder, M. E., Pang, I. H., Duronio, R. J., Gordon, J. I., Sternweis, P. C. & Gilman, A. G. (1991). Lipid modifications of G protein subunits. Myristoylation of $G_{o\alpha}$ increases its affinity for $\beta\gamma$. *Journal of Biological Chemistry* **266**, 4654–4659.

Luchian, T., Dascal, N., Dessauer, C., Platzer, D., Davidson, N., Lester, H. A. & Schreibmayer, W. (1997). A C-terminal peptide of the GIRK1 subunit directly blocks the G protein-activated K^+ channel (GIRK) expressed in *Xenopus* oocytes. *Journal of Physiology* **505**, 13–22.

Nemec, J., Wickman, K. & Clapham, D. E. (1999). $G\beta\gamma$ binding increases the open time of I_{KACh}: kinetic evidence for multiple $G_{\beta\gamma}$ binding sites. *Biophysical Journal* **76**, 246–252.

Reuveny, E., Jan, Y. N. & Jan, L. Y. (1996). Contributions of a negatively charged residue in the hydrophobic domain of the IRK1 inwardly rectifying K^+ channel to K^+-selective permeation. *Biophysical Journal* **70**, 754–761.

Sakmann, B., Noma, A. & Trautwein, W. (1983). Acetylcholine activation of single muscarinic K^+ channels in isolated pacemaker cells of the mammalian heart. *Nature* **303**, 250–253.

Schreibmayer, W., Dessauer, C. W., Vorobiov, D., Gilman, A. G., Lester, H. A., Davidson, N. & Dascal, N. (1996). Inhibition of an inwardly rectifying K^+ channel by G-protein α subunits. *Nature* **380**, 624–627.

Silverman, S. K., Lester, H. A. & Dougherty, D. A. (1996). Subunit stoichiometry of a heteromultimeric G protein-coupled inward-rectifier K^+ channel. *Journal of Biological Chemistry* **271**, 30524–30528.

Slesinger, P. A., Reuveny, E., Jan, Y. N. & Jan, L. Y. (1995). Identification of structural elements involved in G protein gating of the GIRK1 potassium channel. *Neuron* **15**, 1145–1156.

Smith, M. A. & Ashford, M. L. (1998). Mode switching characterizes the activity of large conductance potassium channels recorded from rat cortical fused nerve terminals. *Journal of Physiology* **513**, 733–747.

Spauschus, A., Lentes, K. U., Wischmeyer, E., Dissmann, E., Karschin, C. & Karschin, A. (1996). A G-protein-activated inwardly rectifying K^+ channel (GIRK4) from human hippocampus associates with other GIRK channels. *Journal of Neuroscience* **16**, 930–938.

Sui, J. L., Chan, K. W. & Logothetis, D. E. (1996). Na^+ activation of the muscarinic K^+ channel by a G-protein-independent mechanism. *Journal of General Physiology* **108**, 381–391.

Sui, J. L., Petit-Jacques, J. & Logothetis, D. E. (1998). Activation of the atrial KACh channel by the $\beta\gamma$ subunits of G proteins or intracellular Na^+ ions depends on the presence of phosphatidylinositol phosphates. *Proceedings of the National Academy of Sciences of the USA* **95**, 1307–1312.

Vivaudou, M., Chan, K. W., Sui, J. L., Jan, L. Y., Reuveny, E. & Logothetis, D. E. (1997). Probing the G-protein regulation of GIRK1 and GIRK4, the two subunits of the KACh channel, using functional homomeric mutants. *Journal of Biological Chemistry* **272**, 31553–31560.

Vorobiov, D., Levin, G., Lotan, I. & Dascal, N. (1998). Agonist-independent inactivation and agonist-induced desensitization of the G protein-activated K^+ channel (GIRK) in *Xenopus* oocytes. *Pflügers Archiv* **436**, 56–68.

Wickman, K. & Clapham, D. E. (1995). Ion channel regulation by G proteins. *Physiological Reviews* **75**, 865–885.

Wickman, K. D., Iniguez-Lluhl, J. A., Davenport, P. A., Taussig, R., Krapivinsky, G. B., Linder, M. E., Gilman, A. G. & Clapham, D. E. (1994). Recombinant G-protein $\beta\gamma$-subunits activate the muscarinic-gated atrial potassium channel. *Nature* **368**, 255–257.

Yamada, M., Inanobe, A. & Kurachi, Y. (1998). G protein regulation of potassium ion channels. *Pharmacological Reviews* **50**, 723–757.

Zhou, J. Y., Potts, J. F., Trimmer, J. S., Agnew, W. S. & Sigworth, F. J. (1991). Multiple gating modes and the effect of modulating factors on the microI sodium channel. *Neuron* **7**, 775–785.

Acknowledgements

This work was supported by grants from the National Institutes of Health (GM 56260; N.D.) and USA–Israel Binational Scientific Foundation (96-00201; N.D.). We are grateful to Professor Alfred Gilman (University of Texas, Dallas) for advice and encouragement, and to Professor Ilana Lotan and Dr Dafna Singer-Lahat (Tel Aviv University), Professor Henry A. Lester (California Institute of Technology) and Professor Wolfgang Schreibmayer (Graz University, Austria) for discussions and for critical reading of the manuscript.

Corresponding author

N. Dascal: Department of Physiology and Pharmacology, Sackler School of Medicine, Tel Aviv University, Ramat Aviv 69978, Israel.

Email: dascaln@post.tau.ac.il